NASA Contractor Report 3128

Initial Conceptual Design Study of Self-Critical Nuclear Pumped Laser Systems

Richard J. Rodgers

CONTRACT NAS1-14329
APRIL 1979

NASA

NASA Contractor Report 3128

Initial Conceptual Design Study of Self-Critical Nuclear Pumped Laser Systems

Richard J. Rodgers
United Technologies Research Center
East Hartford, Connecticut

Prepared for
Langley Research Center
under Contract NAS1-14329

National Aeronautics
and Space Administration

**Scientific and Technical
Information Office**

1979

TABLE OF CONTENTS

SUMMARY

An analytical study of self-critical nuclear pumped laser system concepts was performed. Primary emphasis was placed on reactor concepts employing gaseous uranium hexafluoride (UF_6) as the fissionable material. Relationships were developed between the key reactor design parameters including reactor power level, critical mass, neutron flux level, reactor size, operating pressure, and UF_6 optical properties. The results were used to select a reference conceptual laser system configuration.

In the reference configuration, the 3.2 m^3 lasing volume is surrounded by a graphite internal moderator and a region of heavy water. Results of neutronics calculations yield a critical mass of 4.9 kg U^{235} in the form of $^{235}UF_6$. The configuration appears capable of operating in a continuous steady-state mode. The average gas temperature in the core is 600 K and the UF_6 partial pressure within the lasing volume is 0.34 atm.[1]

Laser transitions requiring average fission power densities less than approximately 10^3 W/cm^3 for excitation are most attractive. Operation at wavelengths greater than approximately 400 nm may be required because of limitations imposed by the opacity of gaseous UF_6. Further research directed toward identification of UF_6 compatible lasing transitions is recommended.

[1] 1 atm = 1.013×10^5 Pa.

RESULTS

1. Initial investigation of self-critical nuclear pumped laser concepts has resulted in definition of a reference nuclear pumped laser reactor having the following characteristics: fifty-one unit laser cells, each having a diameter of 20 cm and a length of 200 cm located within a heavy water/graphite reflector moderator; critical mass of 4.9 kg ^{235}U; lasing region gas temperature of 600 K; UF_6 partial pressure of 0.34 atm; total fission power level of 100 MW; fission power density of 31 W/cm^3; and neutron flux of 7×10^{14} n/cm^2-s.

2. Substitution of beryllium for the heavy water as the reflector-moderator material in the reference configuration results in a reduction of the estimated reactor weight from 141,400 to 68,200 kg.

3. The presence in the lasing gas mixture of 0.5 mol percent natural xenon plus an equilibrium amount of Xe^{135} fission product produced at a neutron flux of 10^{15} n/cm^2-s would cause an increase of approximately 11 percent in the reference configuration clean critical mass value of 4.4 kg.

4. Self-critical nuclear pumped lasers employing gaseous UF_6 have the greatest potential for attractive performance if lasing transitions are used having wavelengths greater than approximately 400 nm, where UF_6 is highly transparent.

5. Efforts should be undertaken to identify candidate lasing systems which are chemically and optically compatible with UF_6, capable of efficient operation with excitation levels less than approximately 1 kW/cm^3, and capable of achieving overall efficiency greater than approximately 5 percent.

INTRODUCTION

Self-critical nuclear pumped lasers are one of several possible nuclear pumped laser types currently being studied. This type of laser if proven feasible offers the possibility of very high power operation in a continuous steady-state mode. Possible applications for such lasers include space power generation, space power transmission, and space propulsion.

In self-critical systems it is necessary to select a reactor geometry which meets both the nuclear criticality requirements and the laser optical configuration requirements of the system. In general, cavity reactor configurations are designed having approximately spherical geometry or cylindrical geometry with length-to-diameter of approximately one. This generally results in good neutron economy and leads to systems having low critical mass. High power lasers have been designed in many configurations, some of which are highly two-dimensional and thus unattractive for self-critical nuclear pumping.

Self-critical nuclear pumped laser concepts may use fissionable material in solid, liquid, or gaseous form. A high energy (10 to 100 MJ) nuclear pumped carbon monoxide laser system concept is described in Ref. 1. This system concept utilized thin uranium or uranium oxide foils as fissionable material. Power deposition in systems employing coatings or foils is usually limited by heat transfer within the fissionable material.

Candidate lasers utilizing liquid uranium compounds are described in Refs. 2 and 3. Liquid nuclear pumped lasers appear to solve the heat transfer problems inherent with coating and foil systems. However, neutron damage to the uranium compounds and medium inhomogenities appear to be problems for liquid systems. Recent investigations of lasers using gaseous UF_6 as the fissionable material are described in Refs. 4 and 5. Gaseous systems provide a means for deposition of fission energy directly in the lasing medium. Volumetric excitation of the lasing medium thus should be more efficient in gaseous systems than in systems employing coatings or foils.

The objective of this study was to formulate an initial conceptual design of a gaseous UF_6 reactor configuration for application as a high power nuclear pumped laser. A reference reactor configuration was selected based on results of analyses of criticality, gas flow path, and energy removal considerations. A portion of the study was directed toward scoping of system weight, gas handling and reactor coolant systems based on calculated energy removal requirements for a reference configuration. Discussion of the study results is presented herein.

SELF-CRITICAL DNPL REACTOR DESIGN CHARACTERISTICS

The self-critical DNPL reactor concept requires that the reactor configuration be designed such that parasitic neutron capture of reactor component materials is small. This will permit a low critical mass of nuclear fuel, which enhances the potential performance of the system. For this study, emphasis was placed on use of enriched gaseous UF_6 (93.5% U-235) fuel which is mixed with a gaseous lasing medium in the reactor. The fissioning of the nuclear fuel provides a mechanism to continuously deposit energy in a large lasing volume through fission fragment interaction.

The self-critical UF_6 gaseous core laser reactor has a fuel mixture which is typically composed of three distinct components with unique functions to perform. First, UF_6 must be present in sufficient quantity to produce a sustained fission reaction and thereby to provide the energy source to pump a large volume of the lasing gas mixture. Second, a host gas such as He, Ne, or Ar is present as the dominant energy storage member. The host gas possesses high excitation and ionization energy levels which are populated in the host gas by interaction with high energy fission products. Third, a lasing gas is needed, such as Xe, which is present in small quantities. Energy is transferred by collisions between the excited and ionized host species and lasing gas with the creation of excited and/or ionized states of the lasing gas. Lasing then occurs as the lasing gas radiatively relaxes between energy levels corresponding to its characteristic wavelengths.

An important parameter relative to the lasing system is the neutron flux level required to induce efficient laser action. The flux level required determines the overall reactor power level of a self-critical system. The characteristics of several DNPL laser experiments (Refs. 6 through 13) are listed in TABLE I. The pumping for the configurations in TABLE I was provided using either a boron-10 coating or uranium -235 foil on the inner wall of the laser cell. Neutrons incident on the coatings or foil result in primary particles (reaction products or fission products) being emitted from the inner wall surface into the lasing media. The interaction of these particles creates secondary electrons which both ionize and excite the lasing media. The effective "useful thickness" of the pumped region is determined by the distance from the wall that the primary particle travels as it slows down via collisions. Another technique is to use ^3He gas mixed with the lasing gas. This provides a volumetric energy source when neutrons are incident on the gas mixture. However, the effective "useful thickness" depends upon the penetrating distance of the incident neutrons and the range of the primary reaction products in the gas mixture. The full advantage of high power nuclear pumped laser systems occurs when fission energy is volumetrically created within the lasing medium and the neutron source is not external to the laser cell. This is a characteristic of a self-critical DNPL reactor system and it increases the "useful thickness" and, hence, volume of the pumped lasing region. The data in TABLE I indicate that the lasing threshold neutron flux level is in the range of 10^{15} to 10^{17} n/cm^2-s with the lowest

threshold to date being 4×10^{14} n/cm^2-s for mixtures of He-CO and He-CO_2 (Ref. 9). Research is in progress to identify DNPL systems with lower threshold flux levels. Such systems would be highly attractive for use in a self-critical UF_6-fueled reactor with the lasing medium intimately combined in the nuclear core because the total power level could be reduced.

Fission products transfer kinetic energy to the lasing medium by direct interaction which results in excitation and ionization of the lasing species. The energy required to produce an ion pair in rare gases, as the fission product slows down, is similar to that for energetic electrons. This results because the ionization and excitation is produced principally by secondary electrons which are less energetic than the primary particle. Because of this similarity, it has been suggested (Ref. 14) that studies employing electron-beam pumped laser media composed of atomic gases can yield data applicable to nuclear pumped laser systems. Several experiments (Refs. 15 through 24), are summarized in TABLE II which resulted in laser action in the visible portion of the wavelength spectrum. Based on the data in TABLE II, indications are that high threshold power densities for XeF and KrF are necessary before lasing occurs. Such systems are considered unattractive for self-critical DNPL reactor applications because of the high excitation threshold requirements.

Neutronics Considerations

One objective of the conceptual design study is to establish a range of operating characteristics over which such a reactor system might function. The study was performed under the ground rules that the reactor operates at a steady-state power level and that the reactor core will use fissioning UF_6 gas with operating pressure less than 10 atm and gas temperature in the range of 350 to 700 K.

To determine a set of operating conditions for the self-critical DNPL reactor for sizing purposes, parametric relationships were derived between several reactor variables. Included were relationships between total reactor power, power density, neutron flux level, U-235 mass, U-235 density, and U-235 pressure. Use of these relationships allowed rapid assessment of the effect on reactor design characteristics of changes in parameter values.

The equation which gives total reactor power in megawatts is

$$Q = 8.2 \times 10^{-20}\left(\overline{\sigma}_F \cdot \rho^{U\text{-}235} \cdot \phi \cdot V\right) \qquad (1)$$

where $\overline{\sigma}_F$ is the U-235 fission cross section in barns, $\rho^{U\text{-}235}$ is the U-235 density in g/cm^3, ϕ is the neutron flux in n/cm^2-s, and V is the fuel volume in cm^3. It was

assumed that 200 Mev of energy per fission event is released and that the Maxwellian spectrum weighted fission cross section for U-235 fuel at a temperature of 600 K is given by

$$\overline{\sigma}_F = 0.886\,\sigma_{F_o}\left(\frac{293}{600}\right)^{\frac{1}{2}} = 360 \text{ barns} \qquad (2)$$

where $\overline{\sigma}_{F_o}$ = 582 barns (U-235 fission cross section at T = 293 K). The calculations also assumed that uniform properties exist throughout the fuel region. The relationship between key reactor operating conditions is given in Fig. 1. The results indicate the inter-relationship of the fissioning mass of U-235, thermal neutron flux level, and total reactor power for an average fuel temperature of 600 K. The probable operating region of interest is indicated in Fig. 1 as having a U-235 critical mass of between 1 and 10 Kg and neutron flux level between 10^{14} and 10^{16} n/cm^2-s. This flux range is within that where laser action has been produced in several recent experiments (see TABLE I and Refs. 6 through 13). The corresponding range of total reactor power lies between 3 and 3000 MW.

Additional parametric results are shown in Fig. 2, for a reactor which has a U-235 critical mass of 6.0 kg and gas temperature of 600 K. Figure 2 illustrates the inter-relationship among the power density, neutron flux, and total power, with U-235 density and pressure. A possible extended operating region is indicated for a maximum uranium (U) species partial pressure less than 10 atm, with a more probable operating region limited to U partial pressure less than 1 atm and a minimum U pressure of 0.01 atm.

At the assumed critical mass of 6 kg and temperature of 600 K, the range in U fuel partial pressure between 0.01 and 10 atm corresponds to fuel volumes and, hence, maximum lasing volumes between approximately 120 and 0.12 m^3, respectively.

For the flux range between 10^{14} and 10^{16} n/cm^2-s, the power density ranges between 0.001 and 1.0 kW/cm^3. Results for a different critical mass at the given power and power density can be determined by scaling the pressure and density directly and by scaling the flux inversely with the U-235 mass ratio, $M_{crit}/6.0$ kg. The 6 kg U-235 critical mass is considered typical of that which could be obtained in a gas core reactor system. For this mass of U-235, the range for reactor total power level is between approximately 20 MW and 2000 MW for steady-state systems. If the reactor is sized such that the UF_6 partial pressure is 0.5 atm corresponding to the assumed critical mass of 6 kg, the range of reactor power density required varies between approximately 7 x 10^{-3} kW/cm^3 and 7 x 10^{-1} kW/cm^3. The fuel volume at the 0.5 atm partial pressure value is 2.5 m^3.

An alternative which leads to a major reduction in reactor power level, while achieving a high power density, is to operate systems at high-fuel partial pressure, assuming no significant increase in critical mass occurs. This is possible provided the fuel region continues to have uniform power distribution for the now smaller fuel volumes. The ability to operate efficiently at high pressure also depends on the specific lasing medium used in the reactor and upon the optical absorption coefficient of UF_6 at the specific laser wavelength.

Optical Considerations

In examining potential lasing gas candidates, it is necessary to assess the effect of the UF_6 relative to quenching of laser action at a particular wavelength. The spectral absorption cross section of UF_6 (Ref. 25) is shown in Fig. 3 between 200 and 400 nm. Also indicated are the wavelengths at which potential lasers (KrF, XeBr, I_2, XeF, and N_2) would operate.

Three laser candidate media which operate at wavelengths for which UF_6 absorption is known to be relatively low are the I_2 (342 nm), XF (351, 353 nm), and N_2 (358 nm) lasers. The KrF and XeBr lasers would appear to suffer from too large a UF_6 quenching effect due to the UF_6 optical absorption loss in a self-critical UF_6 DNPL system. Estimates for the maximum efficiency have been made for the I_2 laser (13 percent, Ref. 23) and XF laser (7 percent, Ref. 20).

An I_2 laser operating at 342 nm would appear to have good potential for a UF_6-fueled laser system, since the lasing wavelength occurs in a region where UF_6 has low optical absorption. A series of calculations was performed to relate uranium density and optical path length with values of optical absorption cross section such that optical transmission is 0.85 and 0.95. The results for path lengths of 1, 10, 100, and 1000 cm are shown in Fig. 4. For example, at a uranium density of 10^{-3} g/cm, and path length of 100 cm, 0.95 of the incident energy would be transmitted if the optical absorption cross section were 2×10^{-22} cm^2/atom at any given wavelength. With a knowledge of the gain characteristics for selected transitions, the optical absorption cross section of UF_6 can be used to define a varying U density criteria as a function of wavelength. Wavelengths at which the density is above the nuclear criticality density may be considered candidates for potential DNPL systems.

DESCRIPTION OF REFERENCE DESIGN

Reactor Configuration

A conceptual DNPL reference reactor which is shown in Fig. 5 was selected based on the results of the parametric analyses described in the previous section. A schematic of the reactor configuration is shown in Fig. 6. The core is a matrix of fuel cells. A length-to-diameter (L/D) ratio of approximately one is used for the core. This geometry has a small surface area to volume ratio which reduces neutron leakage from the core. Above and below the fuel cell matrix are regions which contain the laser optics components such as mirrors, beam splitters, etc. A tank of heavy water (0.9975 D_2O) reflector-moderator surrounds the matrix and optics regions. At the top of the D_2O tank, there is a laser power extraction channel with optical windows on the ends. The channel is filled with high pressure deuterium gas to reduce neutron leakage from the core and to provide a transparent light path through the D_2O reflector-moderator.

The core of the reference design consists of a series of modular unit cells in a hexagonal matrix. A cross section of the fuel cell matrix is shown in Fig. 7. The central unit fuel cell operates as a master oscillator. The output of the master oscillator is optically coupled to the other fuel cells which act as single-stage amplifiers connected in parallel. The geometry of the unit cell module is shown in Fig. 8. The module is a hexagonally shaped rod of graphite, with a hollowed-out central cylindrical cavity. The fuel and lasing gas mixture flows through the cavity section of the modules. The cavity cylindrical walls have a nickel coated aluminum liner to isolate the corrosive gas mixture from the graphite structure. The graphite also provides internal neutron moderation and fission density leveling within the core. The unit cells contain cooling channels through which a gas coolant is flowed to convectively remove the energy deposited due to neutron, beta, and gamma heating. The reference reactor configuration has a unit cell length of 200 cm, cavity diameter of 20 cm, and a dimension of 30 cm between any two parallel surfaces of the unit cell. The minimum wall thickness of the graphite cell is 4.5 cm.

The gas mixture within the cells was assumed to be composed primarily of helium and UF_6 in the mole ratio of 10:1. The mixture ratio was selected based on the experimental results of Ref. 14. A gas operating pressure of 10 atm and temperature of 600 K were selected in order to size the radial dimension of the unit cell. The upper lasing states of the gas species are pumped by the interaction of the fission products with the gas mixture. High energy fission products collisionally relax in the gas, resulting in the creation of secondary electrons. The electrons interact with the gas mixture leading to the formation of excited states. The continuous population-depopulation of the excited states leads to cw laser action.

The manner in which the high energy fission products lose energy is such that the median light fission product, possessing a higher initial kinetic energy, has a longer range for slowing down than does the median heavy fission product. The median light fission product range in helium (Ref. 26) was used along with the mixture range-energy relationship (Ref. 27) to calculate the mixture fission product range as a function of pressure and temperature. The results are shown in Fig. 9. For an operating pressure between 5 and 10 atm, and temperature of 600 K, a fission product range of approximately 10 mm (1 cm) results. For a fuel cell in which approximately 95 percent of the kinetic energy of the fission product is to be deposited in the gaseous core volume, a cell radius of approximately 10 cm is required.

The flow path of the fuel mixture is shown in Fig. 10. The fuel is injected into the cell through a slot at the peripheral wall which extends along the entire length of the cavity. The flow enters tangentially to establish a vortex flow within the cell. A major fraction of the flow is withdrawn from the cell via the bypass flow exhaust duct through a perforated plate located in the cylindrical peripheral wall of the fuel cavity. The remainder of the injected flow spirals radially inward and passes out of the fuel cavity through exhaust ports located at the center of the cavity endwalls. By adjusting the injection flow rate, the temperature of the gas in the cavity can be controlled to produce a temperature gradient, and therefore a density gradient whereby the fission energy deposition can be spatially controlled. Use of a confined vortex flow allows the ends of the fuel cavity to be relatively free of obstructions and thus allows a large area for optical extraction.

Neutronics Calculations

A series of neutronics calculations were performed to establish the critical mass and critical fuel density for the reference design (Fig. 6). The calculations were performed for twenty neutron energy groups using the one-dimensional neutron transport theory computer program ANISN (Ref. 28). Neutron cross sections for fast groups were obtained using the HRG code (Ref. 29); for thermal groups using the TEMPEST II code (Ref. 30); with up- and down-scattering probabilities calculated using the SOPHIST-I code (Ref. 31). Cell calculations were performed to obtain neutron spectrum-weighted cross sections for each of four core geometries. The weighted cross sections were used in spherical geometry, critical mass search calculations for which the core geometry was homogenized. The results of these calculations are shown in Figs. 11 and 12. Each of the cores was made up of unit cells having a cross section as shown in Fig. 8. U-235 clean critical masses of 6.6, 2.5, 4.4, and 16.1 kg were calculated for core gas volumes of 0.032, 0.32, 3.2, and 32.0 m^3, respectively. These core volumes correspond to configurations which have 3, 10, 51, and 204 individual cells, having cell lengths of 34, 100, 200, and 500 cm, respectively. The range in critical mass density varied from 0.2 to 5 x 10^{-4} g/cm^3.

For an assumed fuel region temperature of 600 K, the corresponding U-235 partial pressure varied from 42.0 to 0.1 atm for fuel volumes between 0.032 and 32.0 m^3, respectively. The critical mass decreased as the fuel density increased up to a fuel density value of approximately 0.01 g/cm^3 and then the critical mass increased with increasing fuel density. The increase in critical mass results from self-shielding of the fuel in both the central region of each cell as well as in the central section of the cell matrix.

For the reference design (fifty-one cells), a critical mass calculation was performed in which Xe gas was included in the fuel region in an amount equal to 0.5 percent of the He concentration. Also included was the equilibrium Xe^{135} fission product poisoning produced at a neutron flux level of approximately 10^{15} n/cm^2-s, assuming no Xe^{135} fission product removal. The equilibrium amount of Xe^{135} is equal to 29.4 mg. The critical mass was then calculated to be 4.88 kg of U-235, or an approximate 11 percent increase over the clean critical mass obtained with no Xe present. The reference configuration with Xe contained 0.34 atm UF_6 partial pressure based on the assumed fuel temperature of 600 K. The He core partial pressure was assumed to be approximately 10 times greater than the UF_6 pressure, resulting in a total fuel region pressure of 3.8 atm.

A relatively uniform fission energy distribution was obtained across the entire radius of the configuration for the reference core volume of 3.2 m^3. A uniform power density should aid in achieving a large lasing volume within each fuel cavity. Results of the fission energy distribution calculations are shown in Figs. 13 and 14 for the four core volumes. The calculated fission energy distribution within the unit cells for each configuration are shown in Fig. 13. The two largest core volumes (32.0 and 3.2 m^3) exhibit approximately uniform radial fission distribution while the two smallest core volumes (0.32 and 0.032 m^3) exhibit evidence of self-shielding in the central portion of the cell. The ratio of fission density at the cell periphery to that at the cell center was calculated to be 1.13 and 1.37 for the fuel volumes of 0.32 and 0.032 m^3, respectively. The calculated fission energy distribution across the entire cell matrix is shown in Fig. 14. The two largest core volumes have a fission distribution which peaks at the center of the matrix, indicating that these fuel regions are relatively transparent to neutrons. The two smallest core volumes exhibit the effect of fuel self-shielding as expected since an individual cell (Fig. 13) of these configurations showed self-shielding. The 3.2 m^3 volume was selected as the reference configuration primarily because it appeared to have the most uniform fission distribution of the four configurations investigated.

The effect of graphite thickness on fission distribution (based on the minimum graphite thickness between cells) was also investigated for the reference volume (3.2 m^3). The results are shown in Fig. 15, for minimum graphite wall thicknesses of 4.5, 9.5, and 14.5 cm. A minimum graphite thickness of 4.5 cm was selected (see Fig. 8) forthe reference design because it resulted in the most uniform fission

density distribution. It is possible that a more uniform fission energy distribution could be obtained by reducing the graphite thickness below 4.5 cm, and thereby also reduce the critical mass. However, the reduction in thickness would probably not significantly effect the reactor cell performance since the overall power density is quite uniform for the 4.5 cm thickness case (see Fig. 14).

The results of clean critical mass calculations are given in TABLE III for the configurations with internal graphite minimum wall thicknesses of 4.5, 9.5, and 14.5 cm with a surrounding heavy water reflector-moderator of 100 cm. The U-235 masses are 4.4, 5.7, and 7.5 kg, respectively, and corresponding UF_6 partial pressures are 0.29, 0.37, and 0.49 atm for a temperature of 600 K. Two additional calculations were performed in which the heavy water reflector-moderator was replaced with a beryllium moderator. Solid moderator materials would be a better choice than heavy water for DNPL reactors designed for space applications. Beryllium thicknesses equal to approximately one and two thermal neutron diffusion lengths (20 and 40 cm) were used in the calculations. The internal graphite wall thickness was held fixed at 4.5 cm as in the reference design. The calculated U-235 critical masses are 7.6 and 6.3 kg for beryllium thickness of 20 and 40 cm, respectively.

Optical Considerations

The reference design cell matrix is shown in Fig. 7. The central cell operates as a master oscillator, and is optically coupled to other amplifier cells as indicated in Fig. 16. The master oscillator is self-excited. The central cell is configured in an unstable resonator geometry which results in the formation of a large donut-shaped beam such that lasing occurs in most of the fuel cavity volume. This increases the utilization efficiency of the fissioning gain medium, and allows high peak powers to be achieved together with good quality beams.

The output beam of the central cell oscillator is split by a series of mirrors located in the lower optics region. The split beams are amplified in parallel within the remaining fuel cavities and then upon leaving the amplifier cells are recombined into a nominal single beam within the upper optics region. The recombined output laser beam exits from the reactor region through the power extraction channel which is located in the top reflector-moderator region (see Fig. 6).

There are advantages of using a laser oscillator-amplifier configuration over that of a more intense all oscillator configuration. The control and design of a low-power oscillator should be simpler than that of an oscillator with high power potential. A low power oscillator can be designed with confinement of excitation to its fundamental mode, and low beam steering sensitivity of the output to misalignment of the resonator mirrors (Ref. 32).

The effect of possible quenching of lasing in the cells by UF_6 absorption was examined based on the parametric results shown in Fig. 4. Calculations were made to estimate the transmittance through a fuel cell for four different configurations. The results are shown in Fig. 17. The reference design configuration (fifty-one cells, each 200 cm in length) will transmit 0.35 or greater of the incident energy for wavelengths with optical absorption cross section less than or equal to 1.5×10^{-21} cm^2/molecule. This value of the cross section would correspond to the minimum of the spectral absorption cross section (see Fig. 3) for UF_6 in the wavelength range of 200 to 400 nm. The possibility exists that the UF_6 is not a broadband absorber such that there may be narrow optical windows in the spectrum of UF_6 at any wavelength. Also, candidate lasing systems (as yet unidentified) which operate at wavelengths greater than 400 nm, would also be attractive if the UF_6 spectral absorption cross section continues to decrease. Unfortunately, quantitative results are not available in this part of the UF_6 spectrum. A determination of UF_6 absorption in this region of the spectrum should be part of the effort to identify potential nuclear pumped laser systems to be developed in conjunction with a self-critical UF_6-fueled reactor.

The fuel cells have optical windows at both ends to provide for containment of the fissioning gas mixture. The windows used in the self-critical DNPL reactor have a requirement that they must be compatible with UF_6 gas at a temperature of 600 K. Preliminary experimental results are reported in the final report for NASA Contract NAS1-14329 concerning the attack by UF_6 on three candidate laser window materials (high-quality fused silica, calcium fluoride, and aluminum oxide). At temperatures up to 700 K for approximately seventeen hours and UF_6 pressure of approximately 1 atm, the aluminum oxide (sapphire) showed good resistance, while the fused silica and calcium fluoride experienced attack. The preliminary results indicate aluminum oxide as the most promising window material at expected operating conditions of temperature and pressure. To reduce window surface reflection losses, anti-reflection coatings or Brewster angle windows are possibilities. With Brewster angle windows the output wave is plane-polarized, with the reflection loss theoretically reduced to zero in the polarization of the beam. The other linear polarization undergoes high reflection and the resulting attenuation eliminates laser buildup in this polarization (Ref. 33).

There is evidence that aluminum oxide windows will maintain high optical transparency in a reactor environment. An absorption band centered at 205 nm, resulting from reactor irradiation, has been annealed out at a temperature of 773 K in the absence of irradiation. Radiation annealing of the 205 nm absorption band also occurred when a specimen of aluminum oxide was re-irradiated with 1.5 MeV electrons (Ref. 34).

An alternative optical configuration would also use an unstable resonator to drive the amplifier cells; however, in this instance, the output of the oscillator would drive several amplifier chains each of which contains several amplifier cells optically connected in series. The amplifier chains are in parallel and the output from each chain would appear in the six cells surrounding the oscillator cell. To promote stable operation of this oscillator-amplifier configuration, it may be necessary to include isolators in the optical chain to prevent radiation emitted by the amplifiers from interferring with the operation of the oscillator. The function of the isolator is to permit the passage of amplified light in one direction only. These are required for high gain systems. The use of a saturable gas in interstage isolators has been demonstrated for a high gain CO_2 amplifier chain (Ref. 35) to prevent early depletion of the population inversion in a pulsed laser.

The optical configuration using single-stage amplifier cells results in a lower energy flux incident on either the windows or window coatings than does the multi-stage amplifier configuration and, therefore, appears to have lower technical requirements on the windows. However, the single-stage configuration does require more complex components to effect beam splitting and beam combining.

Energy Removal Requirements

Calculations were performed to estimate a range of operating characteristics for the reference DNPL reactor. The results are shown in Figs. 18 through 20 for total power density between 10^{-3} and 10^{-1} kW/cm^3 and average fuel temperature of 600 K. The system parameters calculated are total power, average neutron flux, UF_6 and He weight flow rates, fuel cavity gas residence time, and gas flow velocity. Based on a total reactor power of 100 MW, the following characteristics were determined: power density, 0.031 kW/cm^3; neutron flux, 7 x 10^{14} n/cm^2-s; cavity residence time, 0.023 s, UF_6 flow rate, 322 kg/s; He flow rate, 37 kg/s; and cavity flow velocity, 89 m/s.

For a self-critical reactor system, which is operating cw or quasi-cw, a laser efficiency of greater than approximately 5 percent is desirable. A part of the thermal energy deposited in the lasing gases and reactor structure could be used to produce electricity and the remainder rejected via a space radiator. The fuel (UF_6/He) circuit for the reference design operates at a pressure of 3.8 atm and between temperatures of 351 K and 656 K. During the study, Rankine cycle and a Brayton cycle thermal energy conversion cycles were considered. Schematic diagrams which show the important features of the Rankine and Brayton cycles are presented in Fig. 21. The Rankine cycle would use an organic working fluid. The use of an organic fluid offers the potential for good efficiency over the range of cycle temperatures of interest. Cycle efficiencies in the range of 25 to 35 percent (Ref. 36) appear possible at temperatures which correspond to those of the reference laser reactor configuration.

Previous studies (Refs. 37 and 38) have indicated that use of organic Rankine cycles for space applications is technically feasible. For the cycle configuration shown in Fig. 21a an overall efficiency of 30 percent was assumed. If an organic fluid such as Monsanto CP-27 were used the maximum pressure in the cycle would be about 27 atm. In the Rankine cycle thermal energy is rejected via a condenser/radiator which operates at the lowest temperature present in the cycle. For the cycle conditions in Fig. 21a the radiator/condenser must reject heat at 317 K. A large radiator would be needed to dissipate the 63 MW produced at the reference configuration design point.

Details of the Brayton thermal energy conversion cycle for the reference reactor configuration are shown in Fig. 21b. The working fluid used in the cycle is helium. Conversion efficiency of the Brayton cycle would be less than that of the Rankine cycle for the same maximum and minimum cycle temperature values. The estimated efficiency of the simple Brayton cycle in Fig. 20b is only 9 percent. However, approximately 8 MW of electrical power would be produced via the cycle to meet the requirements of pumps and associated equipment of the laser reactor system. In the Brayton cycle, heat is rejected at higher average temperature than in the Rankine cycle. The ability to reject heat at a higher temperature in the Brayton cycle configuration should allow the size of the radiator required to be reduced relative to the Rankine cycle configuration radiator.

Weight Estimates

A major consideration on reducing system size is based on the reflector-moderator used. The heavy water reflector-moderator configuration leads to a smaller U-235 clean critical mass than the beryllium configuration for the 4.5 cm graphite cell thickness. Therefore, it is expected that the laser quenching effect due to the presence of UF_6 in the lasing cell will be less for the heavy water configuration. However, depending upon the lasing medium used, the difference in quenching by UF_6 for the heavy water configuration versus the beryllium configuration may not significantly affect the laser performance. In this situation, the beryllium configuration possesses an advantage in a space power system. This is shown in TABLE IV, wherein several major reactor component weights are given for the heavy water (100 cm) and beryllium (40 cm) configurations.

The principal weight difference is due to the reflector-moderator itself, with approximately 83,400 kg of heavy water versus 39,600 kg of beryllium used in the respective configurations. Because of its larger physical size, the heavy water configuration also requires a heavier pressure vessel (44,100 kg) than a beryllium configuration pressure vessel (19,000 kg). A stainless steel pressure vessel was assumed stressed for a pressure of 25 atm.

Initial estimates of radiator weights were made for both the Rankine and Brayton energy conversion cycle configurations. The radiator specific weights were calculated by extrapolation of the results of the radiator design analyses described in Ref. 39 to the conditions of interest for the reference laser reactor configuration. For the Rankine cycle system, a radiator specific weight of 2645 kg/MW was determined for the radiator operating temperature of 317 K. If the radiator inlet temperatures could be increased to 367 K, a specific weight of 1010 kg/MW results. A specific weight of 240 kg/MW, was determined for the Brayton cycle radiator which operates at an inlet radiator temperature of 539 K. Estimated weight of the Rankine cycle system radiator (Fig. 21a) is 166,000 kg and that of the Brayton cycle system radiator (Fig. 21b) is 19,700 kg. These weight estimates include allowance for the differences in radiator heat load due to the differences in conversion cycle efficiency. Thus, although the Rankine cycle system is significantly more energy efficient than the Brayton cycle system for the specific reference laser reactor configuration, the Brayton cycle system may be more attractive based on radiator weight considerations.

CONCLUDING REMARKS

The self-critical DNPL reactor may be an attractive candidate for a very high power laser system. Principal features of the reactor are the ability to pump a large gaseous lasing volume, self-contained excitation, and the potential for multi-megawatt continuous power output. However, there are important technical questions concerning the feasibility of the DNPL concept which are unresolved, and which require further research. An effort should be continued to identify potential lasing systems which can function in a UF_6 environment. Based on the known UF_6 optical absorption coefficient values in the 200 to 400 nm wavelength range, lasers which operate near the absorption minimum of 340 nm should be sought. Increased efforts should be made to identify systems that will operate at wavelengths longer than 400 nm because of the apparent low absorption in this spectral region. Sufficiently quantitative optical absorption data for UF_6 are not available in this part of the spectrum. Spectroscopic experiments and calculations are needed to quantify the UF_6 spectral absorption. DNPL experiments should continue to be performed in subcritical configurations but with UF_6 added to the lasing cell in quantities which are consistent with the expected range of critical density. It is important to identify laser enhancement or quenching effects due to the presence of UF_6 for specific candidate systems.

The present study was limited to use of UF_6 as a fuel and only two reflector-moderator configurations were considered. Additional calculations should be performed to investigate other fuels, reflector-moderator materials, and geometric configurations.

REFERENCES

1. Tollefsrud, P. B.: A High Energy Flowing Nuclear Laser. Paper Presented at AFOSR/ONR Nuclear Pumped Laser Workshop, April 6-8, 1976, Monterey, CA.

2. Fader, W. J.: Nuclear Pumped Uranyl Salt Laser. Paper Presented at AFOSR/ONR Nuclear Pumped Laser Workshop, April 6-8, 1976, Monterey, CA.

3. Mansfield, C. R., P. F. Bird, and H. H. Helmick: Nuclear Pumped Actinide and Lanthanide Lasers. Paper Presented at IEEE 1977 International Conference on Plasma Science, May 23-25, 1977, Troy, N.Y.

4. Thom, K. and F. C. Schwenk: Gaseous-Fuel Reactor Systems for Aerospace Applications. J. of Energy, Vol. 1, No. 5, Sept.-Oct. 1977.

5. Thom, K., R. J. Schneider, and H. H. Helmick: Gaseous-Fuel Nuclear Research for Multimegawatt Power in Space. International Astronautical Federation, XXVIIIth Congress, Prague, Sept. 25 - Oct. 1, 1977.

6. DeYoung, R. J., W. E. Wells, G. H. Miley, and J. T. Verdeyen: Direct Nuclear Pumping of a Ne-N_2 Laser. Applied Physics Letters, Vol. 28, No. 9, May 1976, pp 519-521.

7. DeYoung, R. J., N. W. Jalufka, and F. Hohl: Nuclear-Pumped Lasing of ^{3}He-Xe and ^{3}He-Kr. Applied Physics Letters, Vol. 30, No. 1, Jan. 1977, pp 19-21.

8. Akerman, M. A. and G. H. Miley: A Helium-Mercury Direct Nuclear Pumped Laser. Applied Physics Letters, Vol. 30, No. 8, April 1977, pp 409-412.

9. Prelas, M. A., M. A. Akerman, F. P. Boody, and G. H. Miley: A Direct Nuclear Pumped 1.45μ Atomic Carbon Laser in Mixtures of He-CO and He-CO_2. Applied Physics Physics Letters, Vol. 31, No. 7, Oct. 1977, pp 428-430.

10. Jalufka, N. W., R. J. DeYoung, F. Hohl, and M. D. Williams: Nuclear-Pumped ^{3}He-Ar Laser Excited by the ^{3}He(n,p)^{3}H Reaction. Applied Physics Letters, Vol. 29, No. 3, Aug. 1976, pp 188-190.

11. McArthur, D. A. and P. B. Tollefsrud: Observation of Laser Action in CO Gas Excited Only by Fission Fragments. Applied Physics Letters, Vol. 26, No. 4, Feb. 1975, pp 187-190.

12. Gudzenko, L. I. and S. I. Yakovlenko: A UF_6+TlF+F_2 Nuclear-Reaction Laser. Soviet Physics-Lebedev Institute Reports, No. 12, Allerton Press, Inc., New York, 1975, pp 11-14.

REFERENCES (Continued)

13. Mansfield, C. R., P. F. Bird, J. F. Davis, T. F. Wimett, and H. H. Helmick: Direct Nuclear Pumping of a ^{3}He-Xe Laser. Applied Physics Letters, Vol. 30, No. 12, June 1977, pp 640-641.

14. Lorents, D. C., M. V. McCusker, and C. K. Rhodes: Nuclear Fission Fragment Excitation of Electronic Transition Laser Media. Proceedings of the Princeton University Conference on Partially Ionized Plasmas Including the Third Symposium on Uranium Plasmas. (Ed. M. Krishnan) NASA Headquarters, Sept. 1976.

15. Fisher, C. H. and R. E. Center: Threshold Power Density Measurements for Electron-Beam Sustained Discharge Excitation of XeF and KrF. Applied Physics Letters, Vol. 31, No. 2, July 1977, pp 106-108.

16. Ault, E. R. , R. S. Bradford, Jr., and M. L. Bhaumik: High-Power Xenon Fluoride Laser. Applied Physics Letters, Vol. 27, No. 7, Oct. 1975, pp 413-415.

17. Burnham, R., F. X. Powell, and N. Djev: Efficient Electric Discharge Lasers in XeF and KrF. Applied Physics Letters, Vol. 29, No. 1, July 1976, pp 30-32.

18. Mangano, J. A., J. H. Jacob, and J. B. Dodge: Electron-Beam-Controlled Discharge Pumping of the XeF Laser. Applied Physics Letters, Vol. 29, No. 7, Oct. 1976, pp 426-428.

19. Mangano, J. A. and J. H. Jacob: Electron-Beam-Controlled Discharge Pumping of the KrF Laser. Applied Physics Letters, Vol. 27, No. 9, Nov. 1975, pp 495-498.

20. Ewing, J. J. and C. A. Brau: Laser Action on the $^2\Sigma^+_{\frac{1}{2}} \longrightarrow {}^2\Sigma^+_{\frac{1}{2}}$ Bands of KrF and XeCl. Applied Physics Letters, Vol. 27, No. 6, Sept. 1975, pp 350-352.

21. McCusker, M. V., R. M. Hill, D. L. Huestis, D. C. Lorents, R. A. Gutcheck, and H. H. Nakano: The Possibility of an Efficient Tunable Molecular Iodine Laser Near 340 mm. Applied Physics Letters, Vol. 27, No. 6, Sept. 1975, pp 363-365.

22. Bradford, R. S., Jr., E. R. Ault, and M. L. Bhaumik: High-Powered I_2 Laser in the 342-mm Band System. Applied Physics Letters, Vol. 27, No. 10, Nov. 1975, pp 546-548.

23. Tellinghuisen, J., A. K. Hays, J. M. Hoffman, and G. C. Tisone: Spectroscopic Studies of Diatomic Noble Gas Halides. II Analysis of Bound-Free Emission from XeBr, XeI, and XeF. J. of Chemical Physics, Vol. 65, No. 11, Dec. 1976, pp 4473-4482.

REFERENCES (Continued)

24. Searles, S. K.: Superfluorescent Laser Emission From Electron-Beam-Pumped Ar-N_2 Mixtures. Applied Physics Letters, Vol. 25, No. 12, Dec. 1974, pp 735-737.

25. DePoorter, G. L. and C. K. Rofer-DePoorter: The Absorption Spectrum of UF_6 from 2000 to 4200 A. Spectroscopy Letters 8 (8), 1975, pp 521-524. Also LASL Report LA-HR-75-792.

26. Reactor Physics Constants. Argonne National Laboratory Report ANL-5800, July 1963.

27. Evans, R. D.: The Atomic Nucleus. McGraw-Hill Book Co., Inc., New York, 1955.

28. Engle, W. W., Jr.: A User's Manual for ANISN, A One-Dimensional Discrete Ordinates Transport Code with Anisotropic Scattering. Union Carbide Corp. Report K-1693, 1967.

29. Carter, J. L.: HRG3 - A Code for Calculating the Slowing-Down Spectrum in the P1 or B1 Approximations. Battelle-Northwest Laboratory Report BNWL-1432, June 1970.

30. Shudde, R. H. and J. Dyer: TEMPEST-II, A Neutron Thermalization Code. North American Aviation Report AMTD-111, Sept. 1960.

31. Canfield, E. H., R. N. Stewart, R. P. Freis, and W. H. Collins: SOPHIST-I, An IBM 709/7090 Code Which Calculates Multigroup Transfer Coefficients for Gaseous Moderators. University of California, Lawrence Livermore Radiation Laboratory Report UCRL-5756, Oct. 1961.

32. Dyer, P. E. and D. J. James: High-Power Mode-locked Tea CO_2 Laser Using an Unstable Resonator. Applied Physics Letters, Vol. 26, No. 6, Mar. 1975, pp 331-334.

33. Bloom, A. L.: Gas Lasers. John Wiley & Sons, Inc., New York, 1968.

34. Palma, G. E. and R. M. Gagosz: Effect of 1.5 MEV Electron Irradiation on the Transmission of Optical Materials. NASA CR-123187, 1971.

35. Lavigne, P., J. L. Lachambre, and J. Gilbert: Gaseous Saturable Isolator for a High Gain CO_2 Amplifier Chain. Applied Physics Letters, Vol. 28, No. 5, March 1976, pp 265-267.

36. Bjerklie, J., and S. Luchter: Rankine Cycle Working Fluid Selection and Specification Rationale. SAE Paper No. 690063, International Automotive Engineering Congress, Detroit, Michigan, Jan. 13-17, 1969.

37. Brouns, R. C., E. C. Krueger, R. E. Niggemann, G. L. Sorenson, F. A. Russo: KIPS, Kilowatt Isotope Power System. Proceedings of the 12th Intersociety Energy Conversion Engineering Conference, Vol. 2, Washington, D.C., August 28 - September 2, 1977.

38. Goodman, M. and W. B. Thomson: A 5-GW_e Nuclear Satellite Power System Conceptual Design. Proceedings of the 13th Intersociety Energy Conversion Engineering Conference, Vol. 1, San Diego, CA., August 20-25, 1978.

39. Rodgers, R. J., T. S. Latham, and H. E. Bauer: Analytical Studies of Nuclear Light Bulb Engine Radiant Heat Transfer and Performance Characteristics. NASA CR-123189, 1971.

LIST OF SYMBOLS

a	Length of side for hexagon fuel cell, cm
$FD/\overline{FD}$	Ratio of fission density to average value of fission density, dimensionless
I/Io	Transmission, dimensionless
L/D	Length-to-diameter ratio of core matrix, dimensionless
ℓ	Fuel cell length, cm
M	Mass, g or kg
M_{crit}	Critical mass, kg
N	Atom number density, cm^{-3}
P	Pressure, atm
Q_T	Total power, MW
R	Radius, cm
R_{cell}	Radius of fuel cell, cm
R_{ff}	Medium-light fission fragment range, mm
R_{hex}	One-half minimum chord length for hexagon cross section, cm
R_{sph}	Radius of core fuel cell matrix in spherical model, cm
T_F	Average fuel mixture temperature, deg K
V_F	Gaseous core volume, m^3
α	Optical absorption cross section, cm^2
λ	Wavelength, nm or Å
ρ	Density, g/cm^3

TABLE I

CHARACTERISTICS OF NUCLEAR PUMPED LASERS

Lasing Medium	Pressure Atm	Wave-Length Å	Thermal Flux Threshold n/cm^2-s	Average Thermal Flux n/cm^2-s	Power Density	Reference Number
$Ne-N_2$ $B^{10}(n,\alpha)Li^7$	0.2	8629 9393 (N)	$1x10^{15}$	$4.8x10^{15}$ (peak)	3.3 w/cm^3	6
^3He-Xe $^3He(n,p)^3H$	0.5	20270 (XEI)	$4x10^{15}$	$6x10^{15}$		7
^3He-Kr $^3He(n,p)^3H$	0.5	25000 (KRI)	$1.1x10^{17}$			7
He-Hg $B^{10}(n,\alpha)Li^7$	0.8	6150 (Hg^+)	$1x10^{16}$	$3.8x10^{16}$ (peak)	0.2 kW/cm^3	8
He-CO $He-CO_2$ $B^{10}(n,\alpha)Li^7$	0.8	14550 (C)	$4x10^{14}$	$2.5x10^{15}$ (peak)		9
^3He-Ar $^3He(n,p)^3H$	1.0	17900 (Ar)	$1.4x10^{16}$	$1.2x10^{17}$		10
CO $U(n,\nu n)FF$	0.1	51000→ 56000 (CO)		$1x10^{17}$ (peak)	2 kW/cm^3	11
$UF_6-TlF-F_2$ $U(n,\nu n)FF$		4000 (Tl)			1-6 W/cm^3	12
^3He-Xe $^3He(n,p)^3H$	0.8	20270 35080 36520 (XEI)		$3x10^{16}$	0.200 kW/cm^3	13

TABLE II

CHACTERISTICS OF E-BEAM PUMPED VISIBLE AND NEAR UV LASERS

Lasing Medium	Wavelength Å	Pressure Atm	Power MW	Power Density Threshold kW/cm^3	Power Density Deposited MW/cm^3	Efficiency (MAX,EST EFF)	Reference Number
$Ar/Xe/NF_3$	3510,3530(XF)	1.0	-	10 20	0.1	0.5%	15
"	"	1.7	0.8	-	0.25	3%	16
$He/Xe/NF_3$	" "	1.0	25	-	25	1%(2-5%)	17
$Ar/Xe/NF_3$	" "	4.0	0.2	-	-	3%(7%)	18
$Ar/Kr/F_2$	2485(KrF)	1.0	-	20	0.1	-	15
"	"	1.5	0.004	40	0.22	0.2%(5-10%)	19
$He/Kr/F_2$	" "	1.0	0.12	-	4.0	0.3%(2-5%)	17
$Ar/Kr/F_2$	" "	3.5	0.08	-	1.3	0.4%	20
Ar/CF_3I	3420(I_2)	2.0	-	-	-	(13%)	21
"	"	10.0	3.6	-	1.7	-	22
Xe/HBr	2818(XeBr)	0.5	0.001	-	-	-	23
Ar/N_2	3577(N_2)	1.0	0.018	-	0.2	0.4%	24

TABLE III

CLEAN CRITICAL MASS CALCULATIONS AT REFERENCE VOLUME

R_{cell} = 10 cm
Length = 200 cm
No. of Cells = 51
Total Volume = 3.2 m^3
T_F = 600 K

Reflector-Moderator (Thickness)	Internal Graphite Moderator (thickness) cm	U-235 Critical Mass, kg	U-235 Density mg/cm^3	UF_6 Pressure, atm
D_2O (100 cm)	4.5	4.4	1.38	0.29
D_2O (100 cm)	9.5	5.7	1.77	0.37
D_2O (100 cm)	14.5	7.5	2.34	0.49
Be (20 cm)	4.5	7.6	2.39	0.50
Be (40 cm)	4.5	6.3	1.95	0.41

TABLE IV

REACTOR GROSS WEIGHT

(See TABLE III for Geometry and Criticality Results)

	Heavy Water Configuration (100 cm) (Kg)	Beryllium Configuration (40 cm) (Kg)
Core		
Graphite	8700	8700
Ni-Al Liner	900	900
Moderator		
Heavy Water or Be	83400	39600
Al Tank	4300	-
Pressure Vessel (25 atm)	44100	19000
Subtotal	141400	68200
Space Radiator (Rankine at 317 K)	166000	166000
Space Radiator (Rankine at 367 K)	58000	58000
Space Radiator (Brayton at 539 K)	19700	19700
TOTAL (Reactor Plus Radiator - Rankine at 317 K)	307400	234200
TOTAL (Reactor Plus Radiator - Rankine at 367 K)	199400	126200
TOTAL (Reactor Plus Radiator - Brayton at 539 K)	161100	87900

VARIATION OF U–235 MASS WITH REACTOR TOTAL POWER

T_F = 600 K

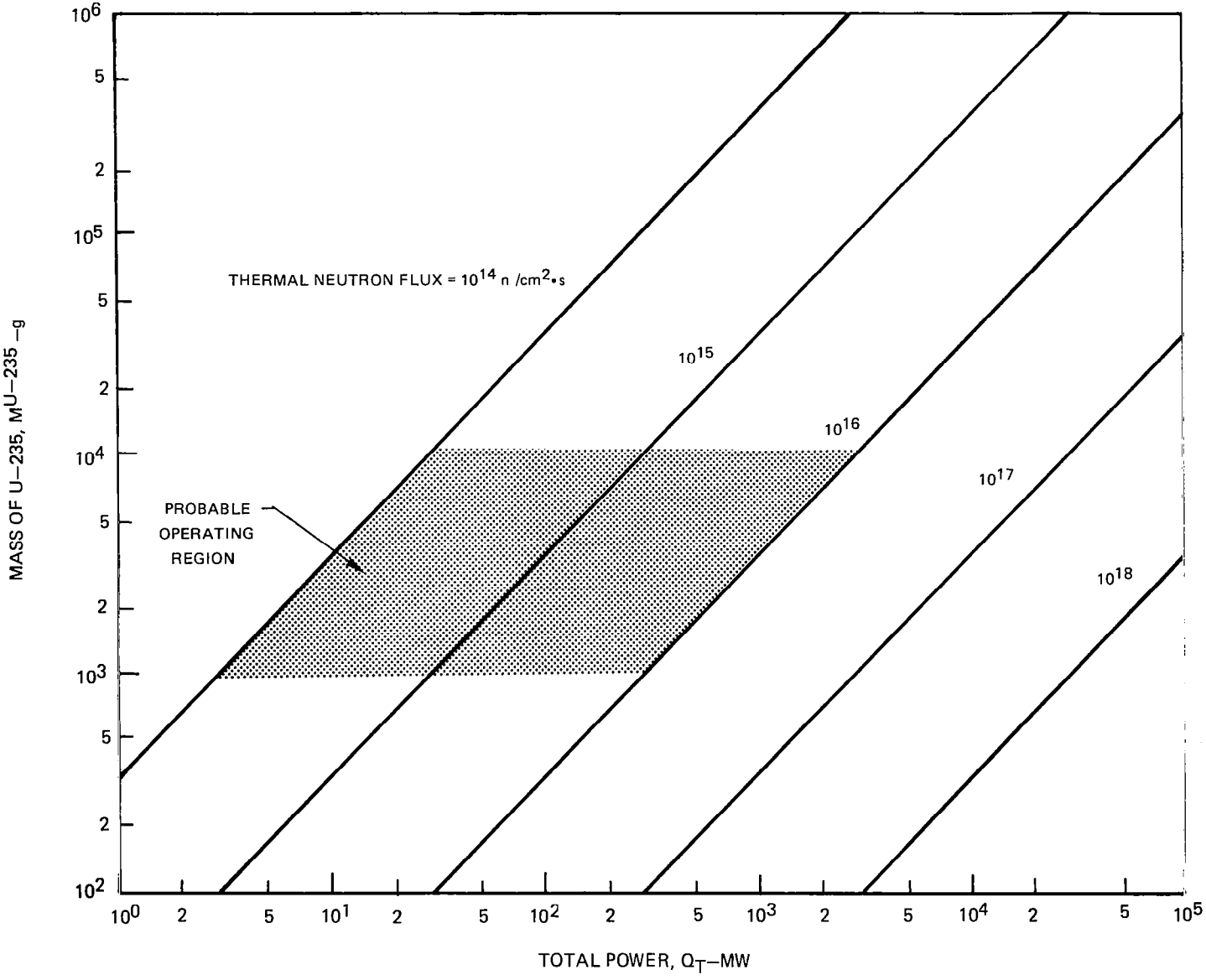

FIG. 1

RELATIONSHIP BETWEEN KEY NUCLEAR PUMPED LASER SYSTEM PARAMETERS

T_F = 600 K

ASSUMED CRITICAL MASS: 6.0 kg

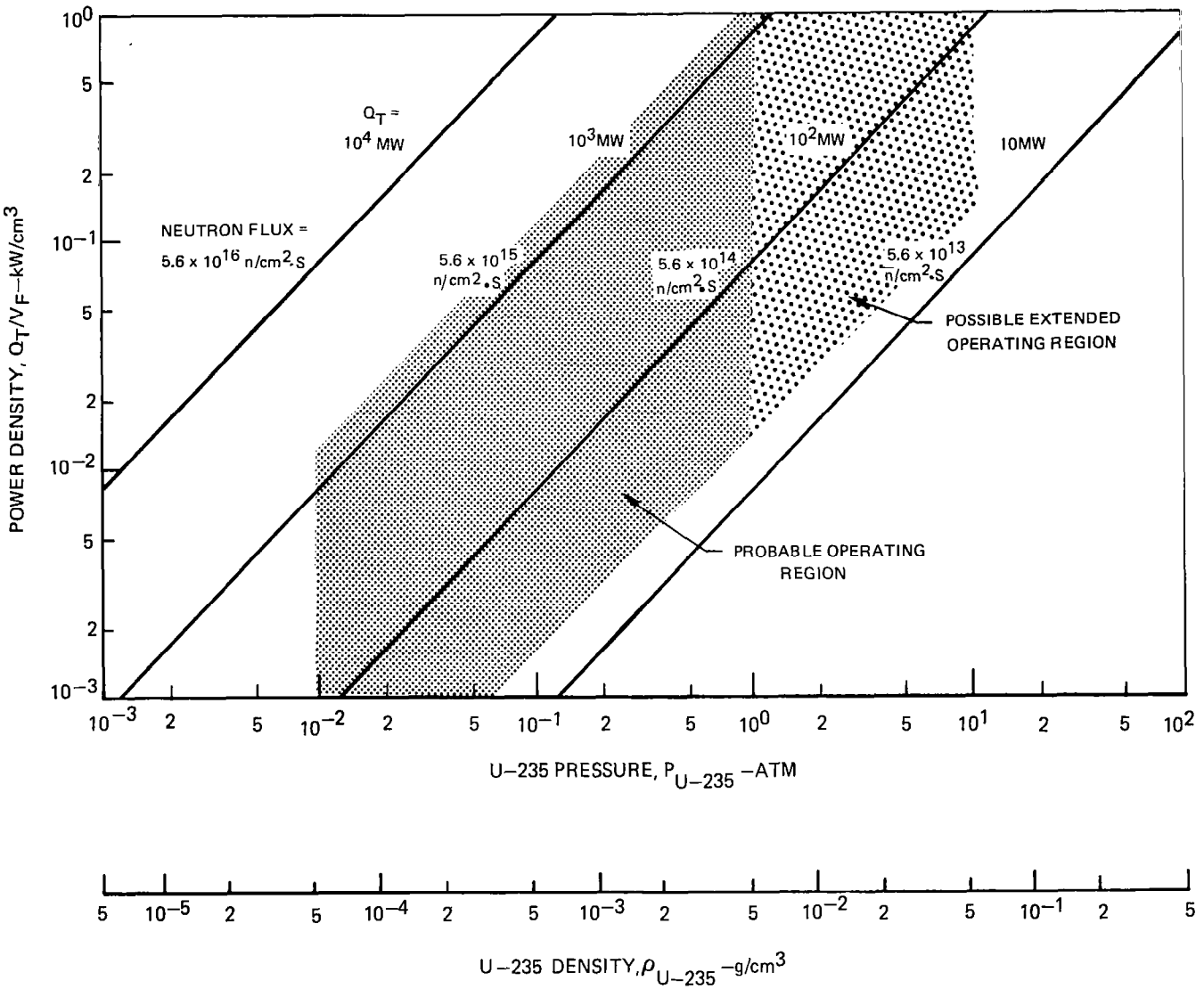

FIG. 2

FIG. 3

VARIATION OF UF_6 ABSORPTION CROSS–SECTION WITH WAVELENGTH

SEE REF. 25

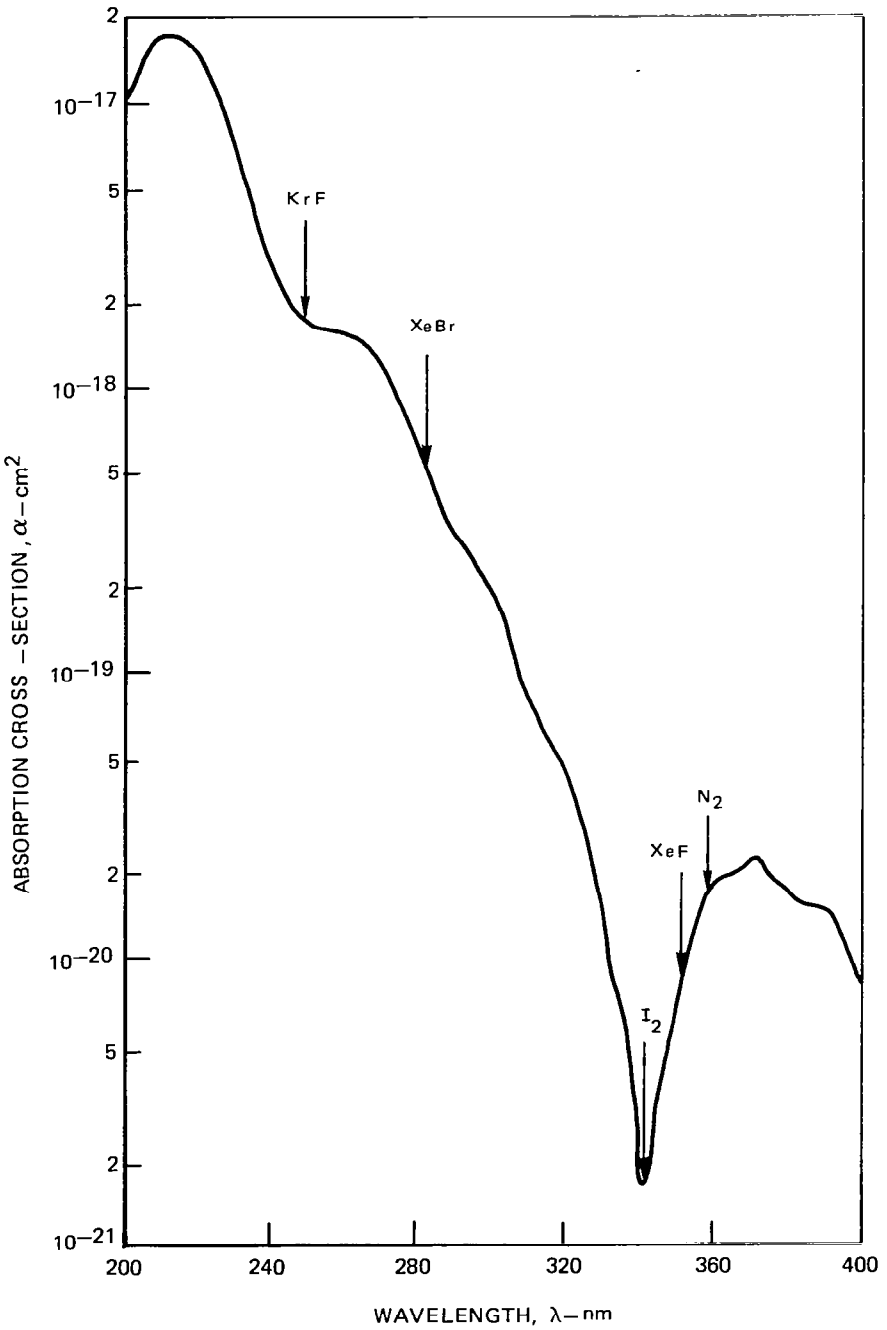

VARIATION OF URANIUM DENSITY WITH OPTICAL ABSORPTION CROSS-SECTION FOR TRANSMISSION BETWEEN 0.85 AND 0.95

TRANSMISSION, I/I_0 = 0.95 (———)
= 0.85 (– – –)

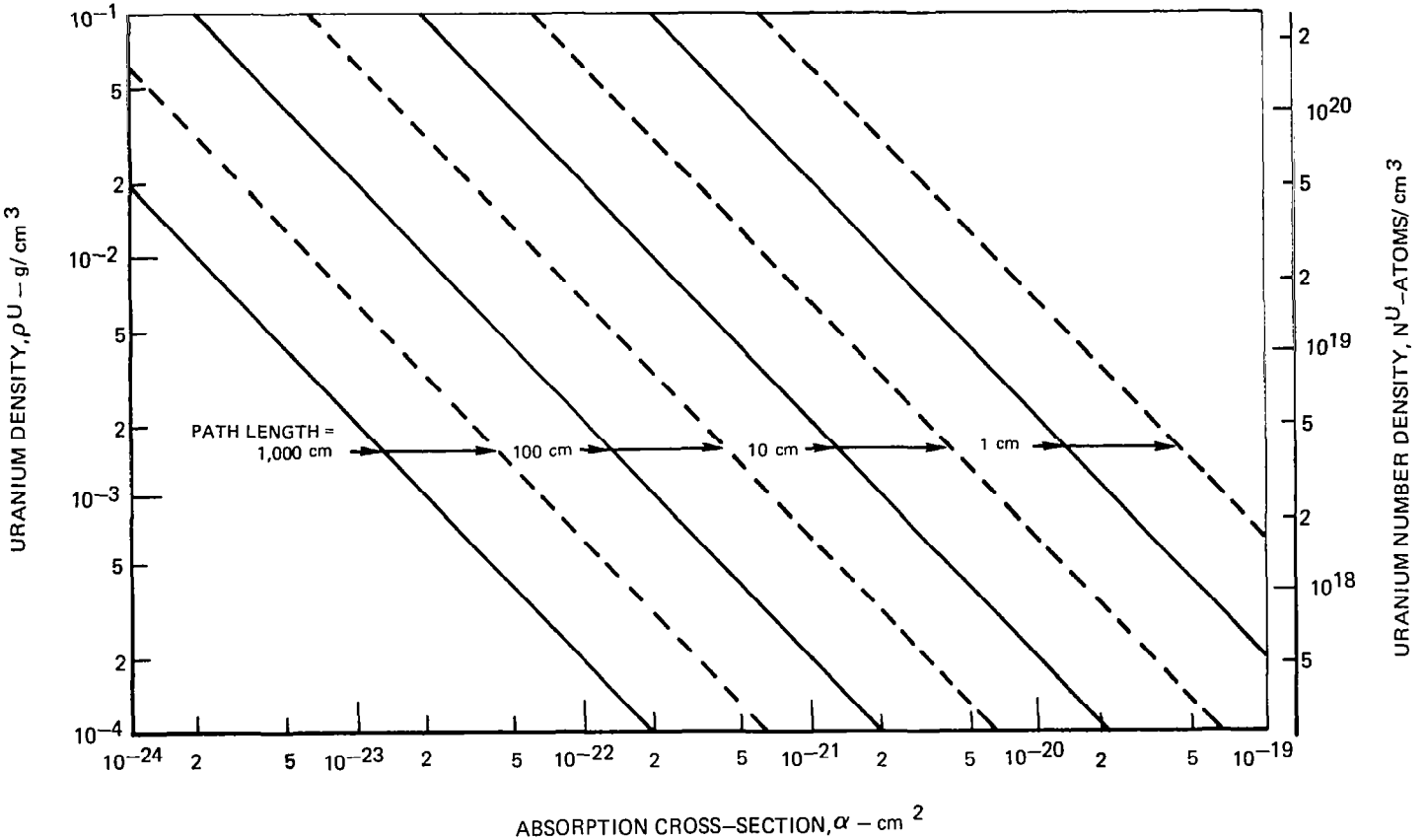

FIG. 4

FIG. 5

CONCEPTUAL UF_6 GASEOUS NUCLEAR PUMPED LASER REACTOR

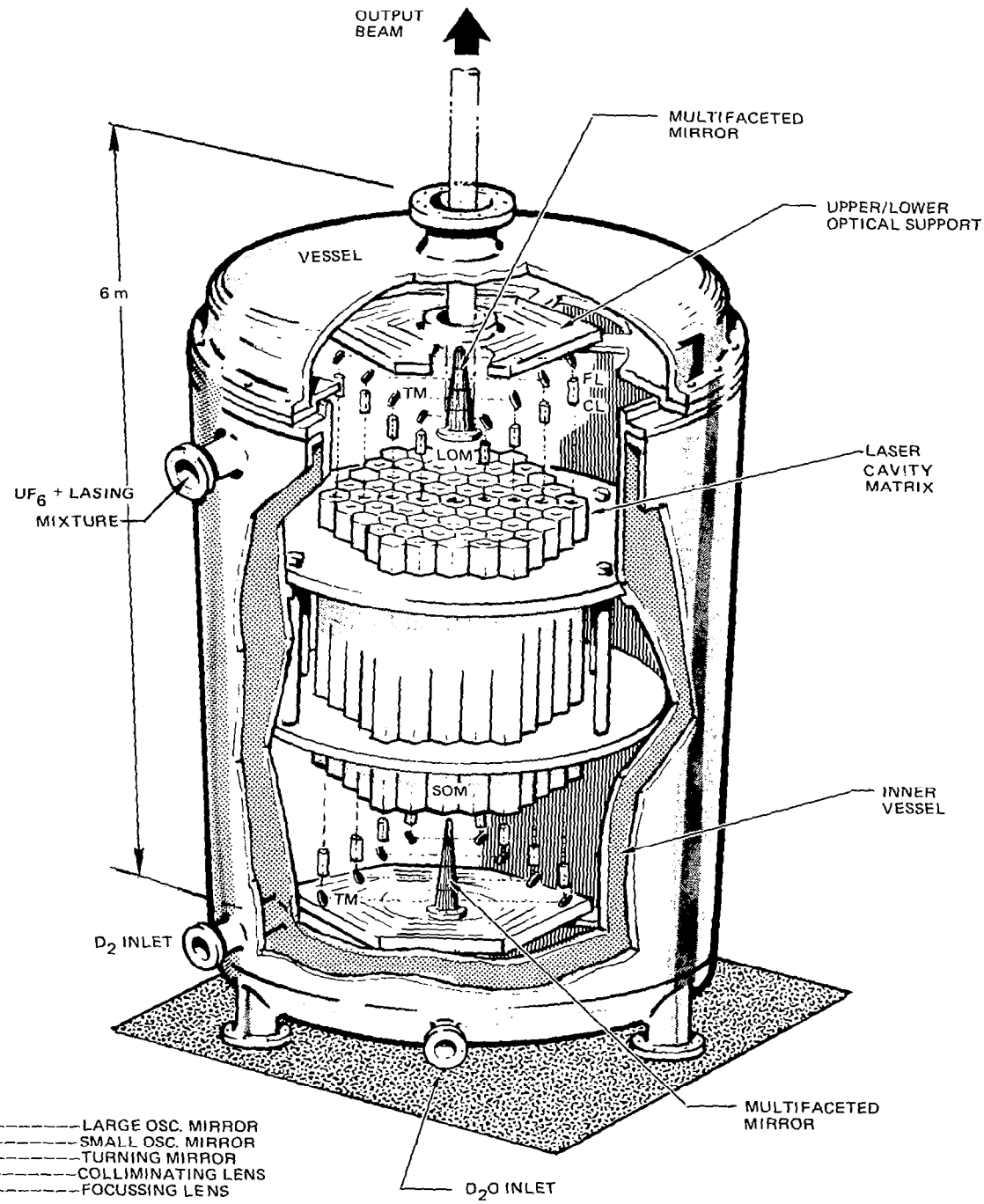

FIG. 6

REFERENCE REACTOR CONFIGURATION FOR UF_6 GASEOUS NUCLEAR PUMPED LASER REACTOR

ALL DIMENSIONS IN CENTIMETERS

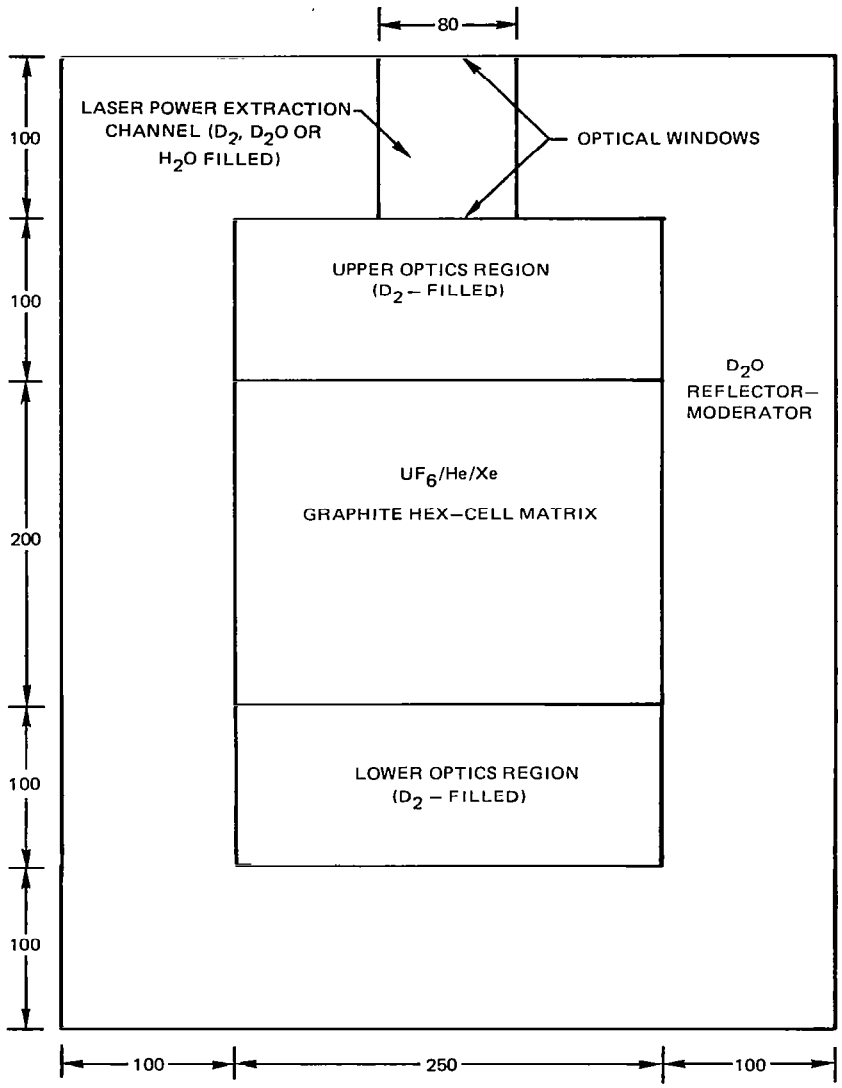

FIG. 7

UF_6 REACTOR LASING CELL MATRIX

MASTER OSCILLATOR DRIVES AMPLIFIER CELLS

X–CODED CELLS ARE SOLID He–COOLED GRAPHITE

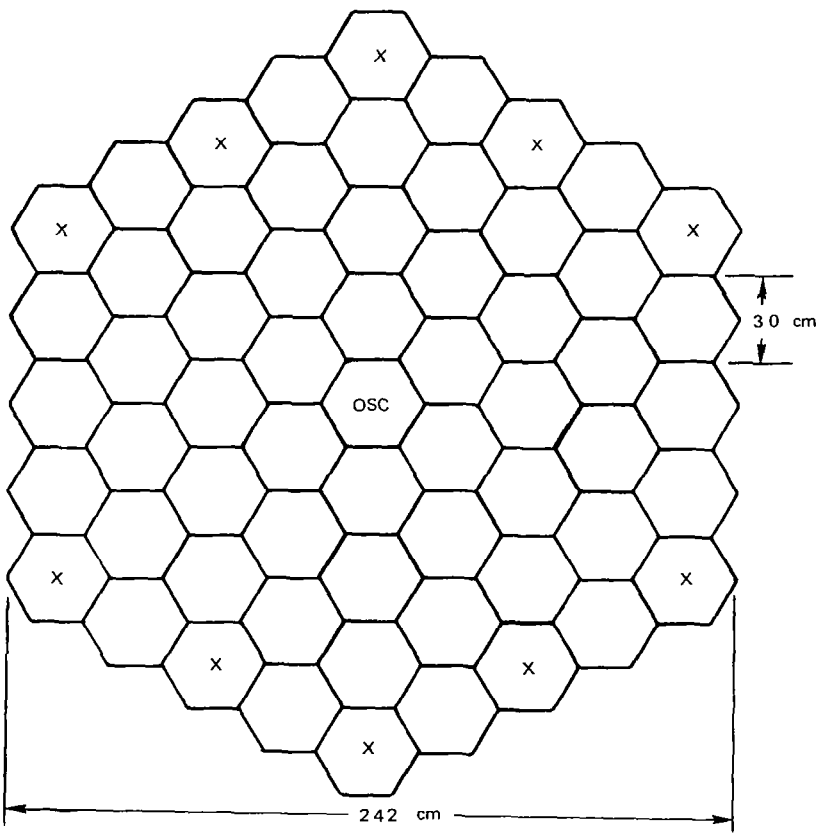

MASTER OSCILLATOR

50 AMPLIFIERS

UNIT FUEL CELL FOR LASING REACTOR MATRIX

REF. CELL LENGTH: 200 cm

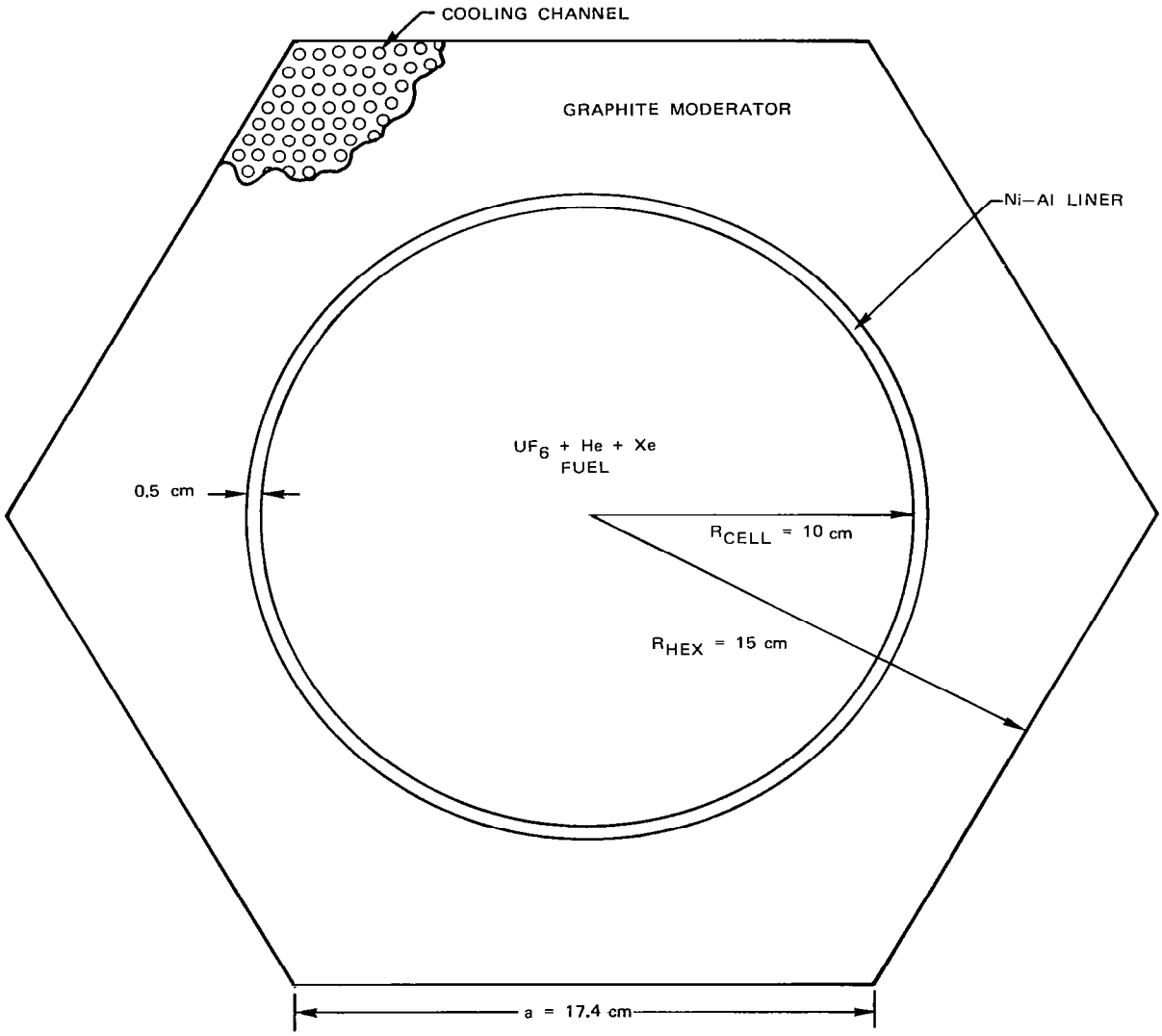

FIG. 9

MEDIAN–LIGHT FISSION FRAGMENT RANGE IN UF_6–He MIXTURE

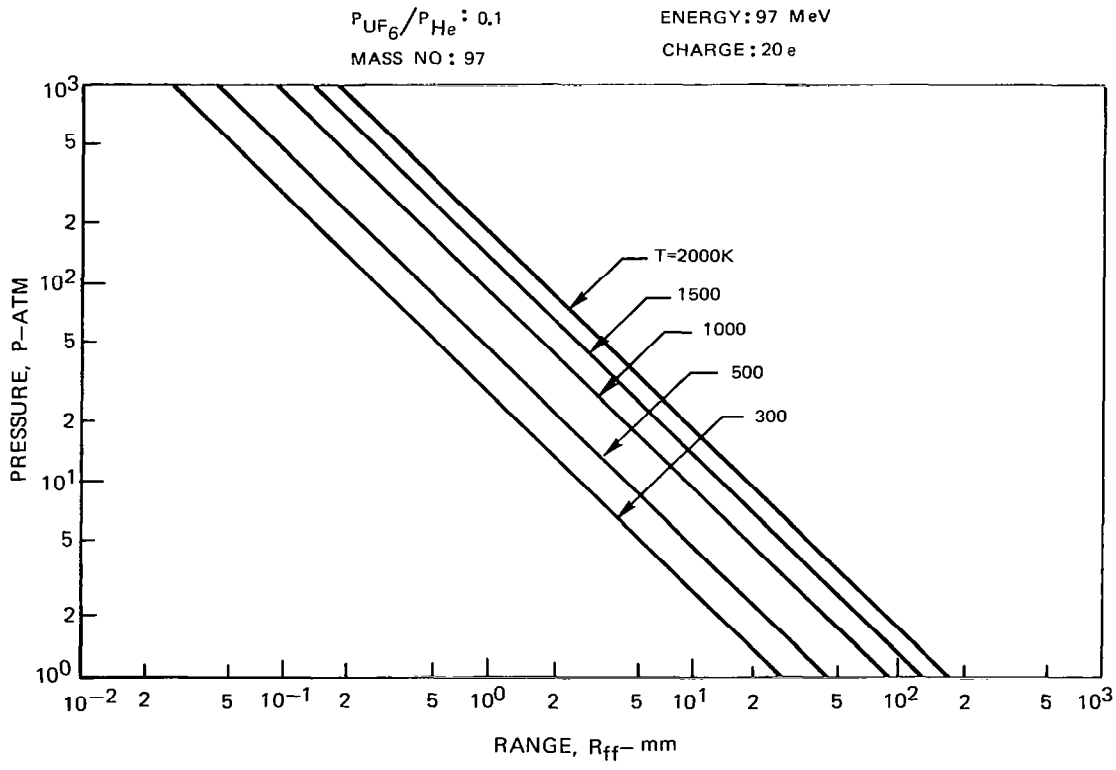

FIG. 10

UF_6 LASER REACTOR FUEL CAVITY FLOW PATH

CAVITY DIAMETER : 20 CM

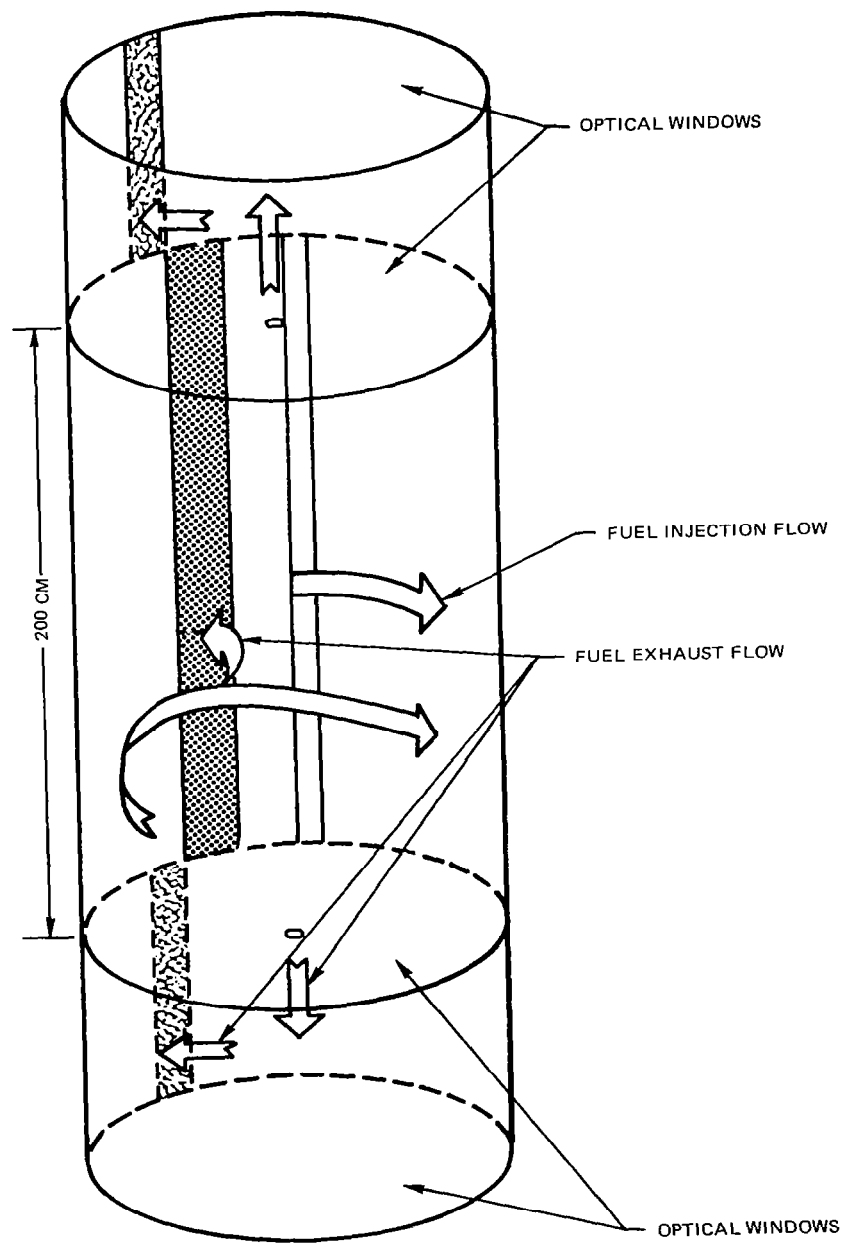

VARIATION OF CALCULATED CLEAN CRITICAL MASS WITH FUEL DENSITY

SEE FIG. 6 FOR GEOMETRY

FUEL MATRIX REGION L/D≈1

FUEL CELL RADIUS = 10 cm

REFERENCE CONFIGURATION INCLUDES 29.4 mg OF Xe^{135} EQUILIBRIUM FISSION PRODUCT POISONING

AND ≈131 g (0.5%) Xe^{NAT} LASING GAS

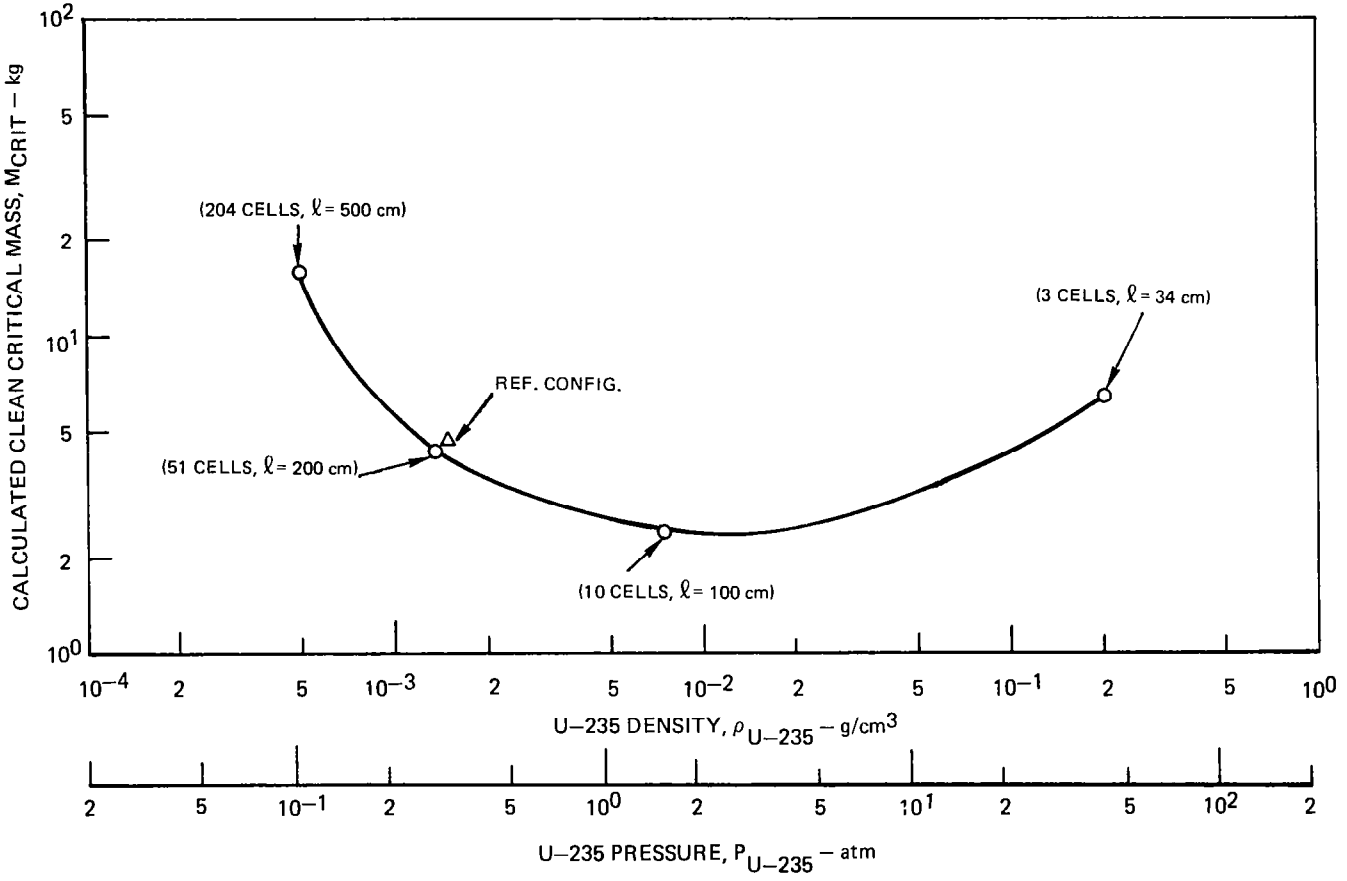

FIG. 11

VARIATION OF CALCULATED CLEAN CRITICAL MASS WITH FUEL REGION VOLUME

SEE FIG. 6 FOR GEOMETRY
FUEL MATRIX REGION L/D≈1
FUEL CELL RADIUS = 10 cm

REFERENCE CONFIGURATION INCLUDES 29.4 mg OF X_e^{135} EQUILIBRIUM FISSION PRODUCT POISONING AND ≈131g (0.5%) X_e^{NAT} LASING GAS

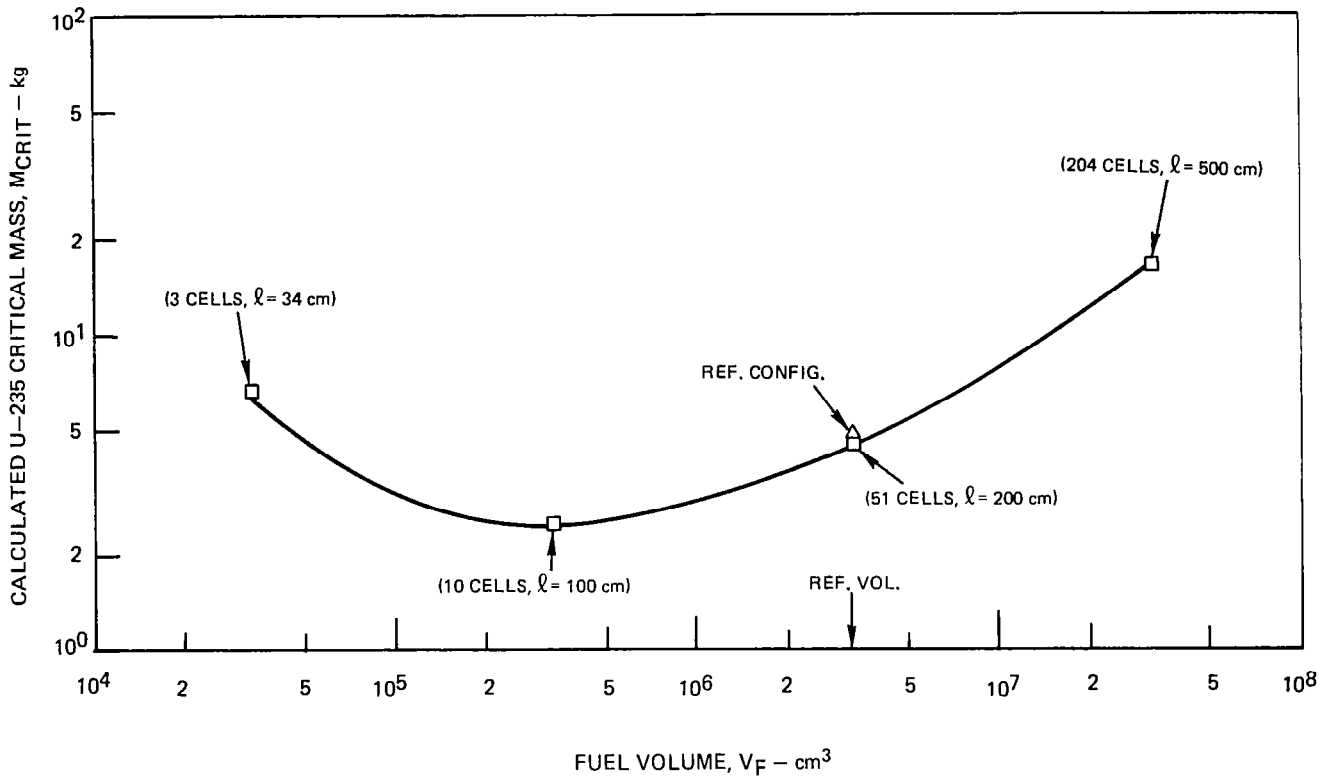

FIG. 12

FIG. 13

VARIATION OF FISSION DENSITY RATIO WITH RADIUS FOR A UNIT CELL IN SEVERAL REACTOR CONFIGURATIONS

SEE FIG. 8 FOR CELL GEOMETRY
SEE FIG. 11 FOR FUEL LOADINGS
CELL RADIUS, R_{CELL} : 10 cm
REF. VOL. : 3.2 m^3

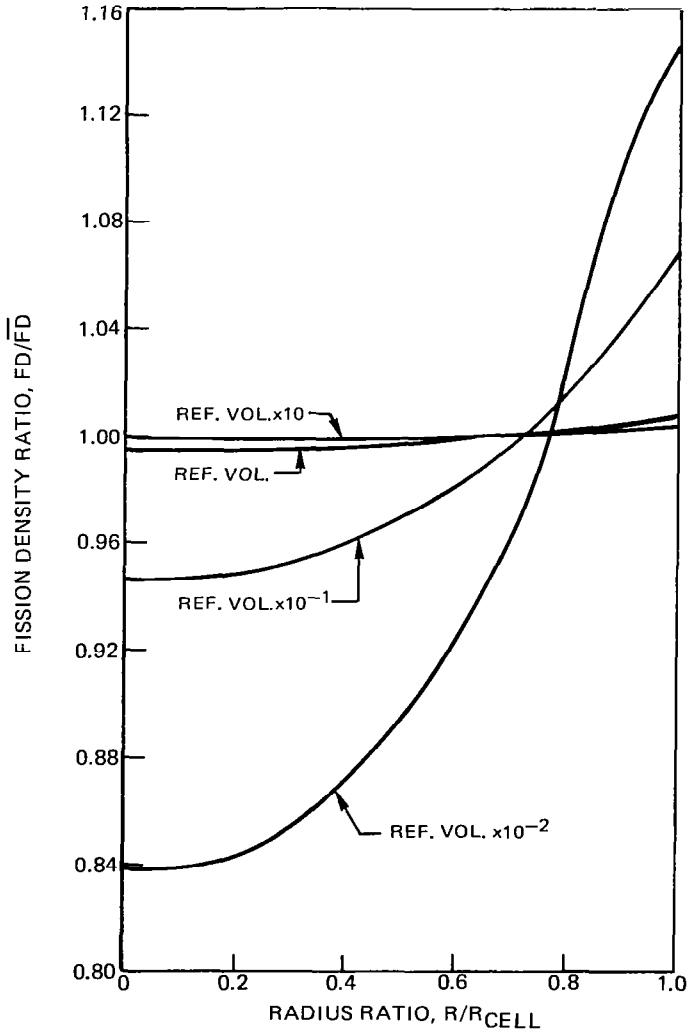

VARIATION OF FISSION DENSITY RATIO WITH SPHERICAL RADIUS OF MATRIX OF FUEL CELLS FOR SEVERAL REACTOR CONFIGURATIONS

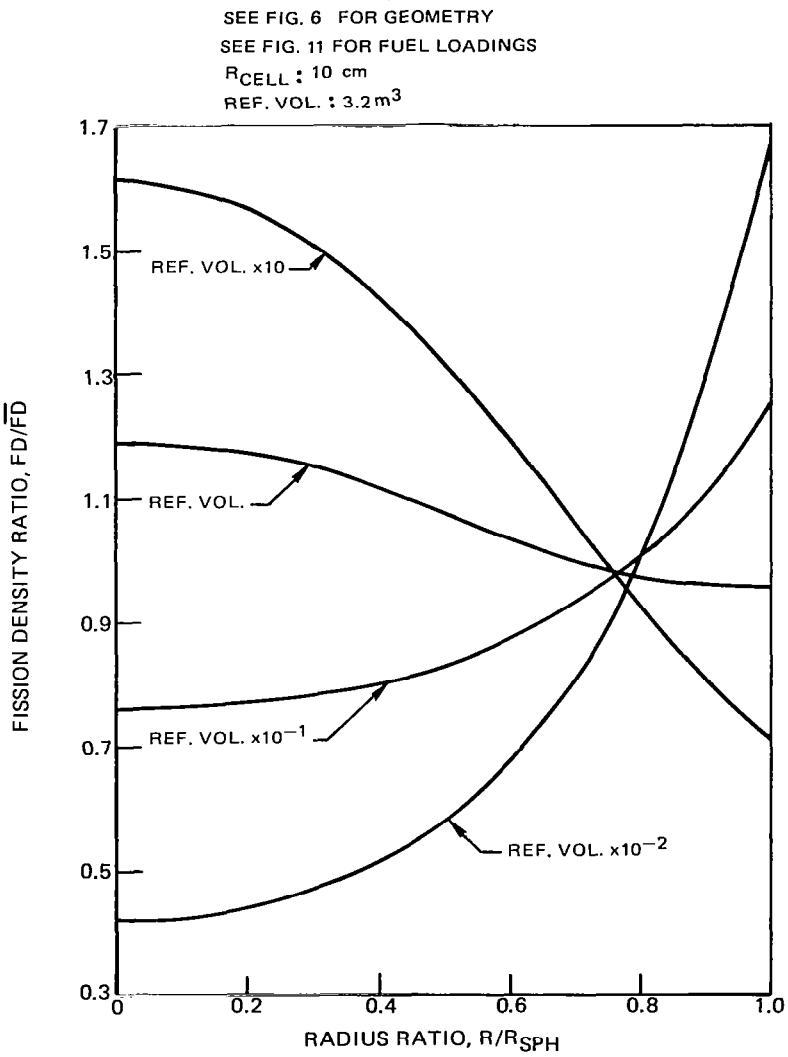

FIG. 15

VARIATION OF FISSION DENSITY RATIO WITH SPHERICAL RADIUS OF MATRIX OF FUEL CELLS FOR DIFFERENT THICKNESSES OF GRAPHITE IN THE CELL CALCULATIONS

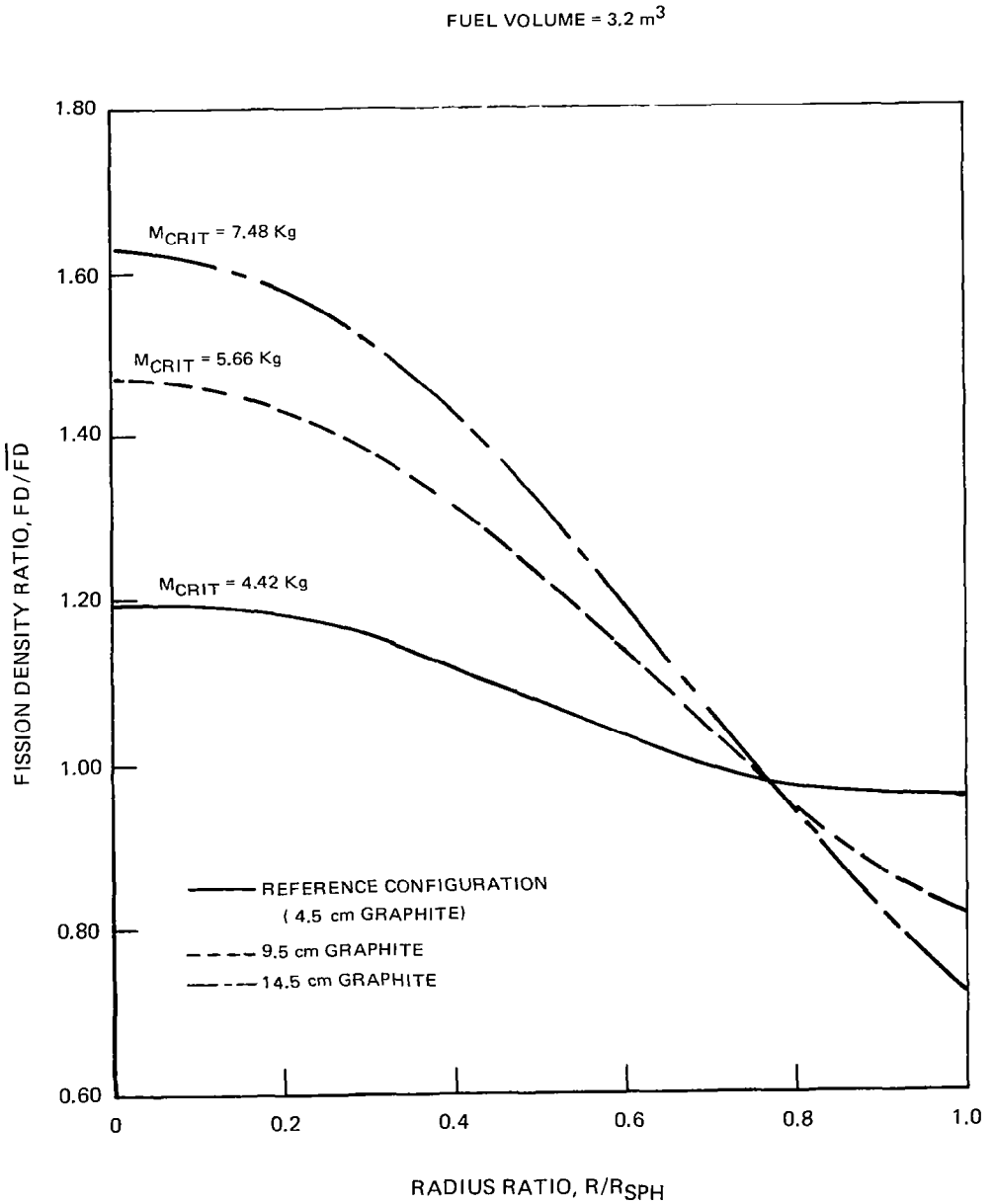

FIG. 16

OPTICAL COMPONENT CONFIGURATION FOR OSCILLATOR–AMPLIFIER NUCLEAR PUMPED LASER

MIRRORS ARE HIGHLY REFLECTIVE DIELECTRIC–COATED
AMPLIFIER WINDOWS HAVE ANTI–REFLECTION COATING
OR CUT AT BREWSTER ANGLE

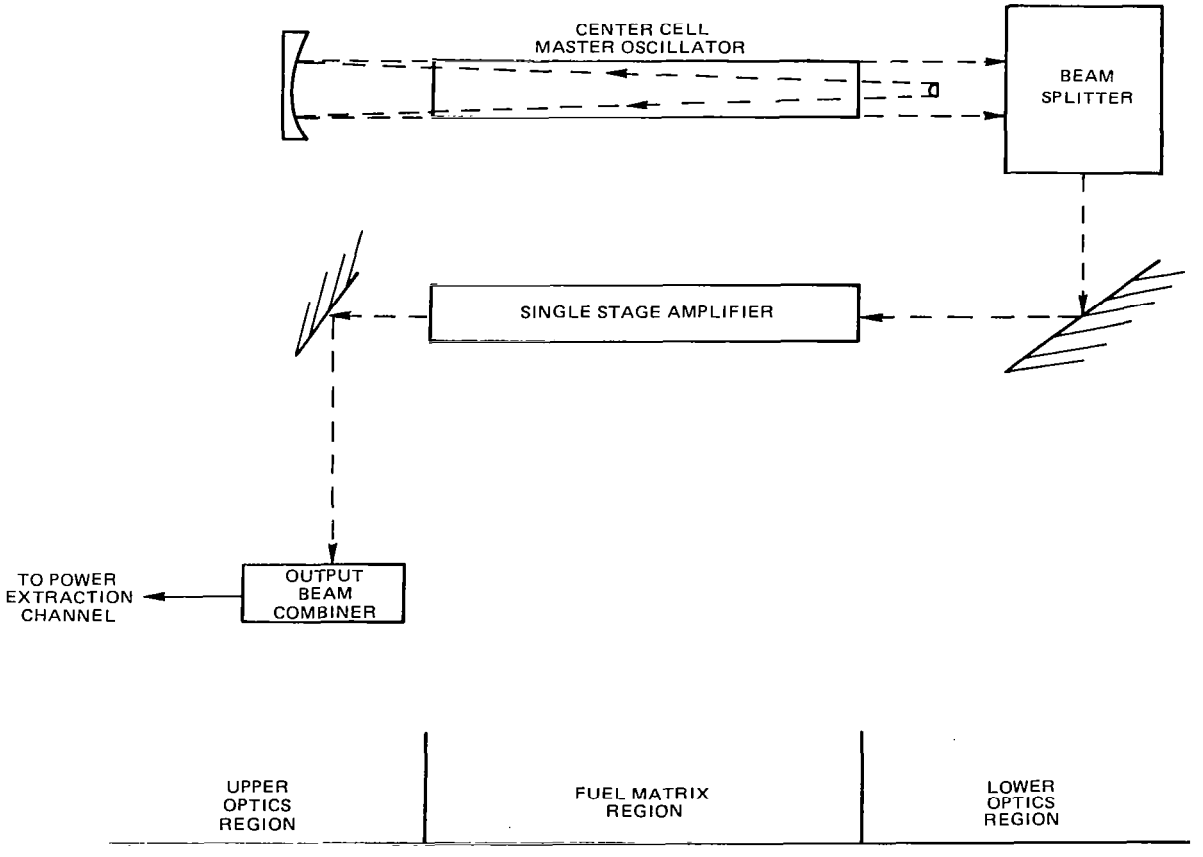

FIG. 17

VARIATION OF OPTICAL ABSORPTION CROSS–SECTION WITH UF_6 PRESSURE

FUEL MATRIX REGION L/D≈1

T_F = 600 K

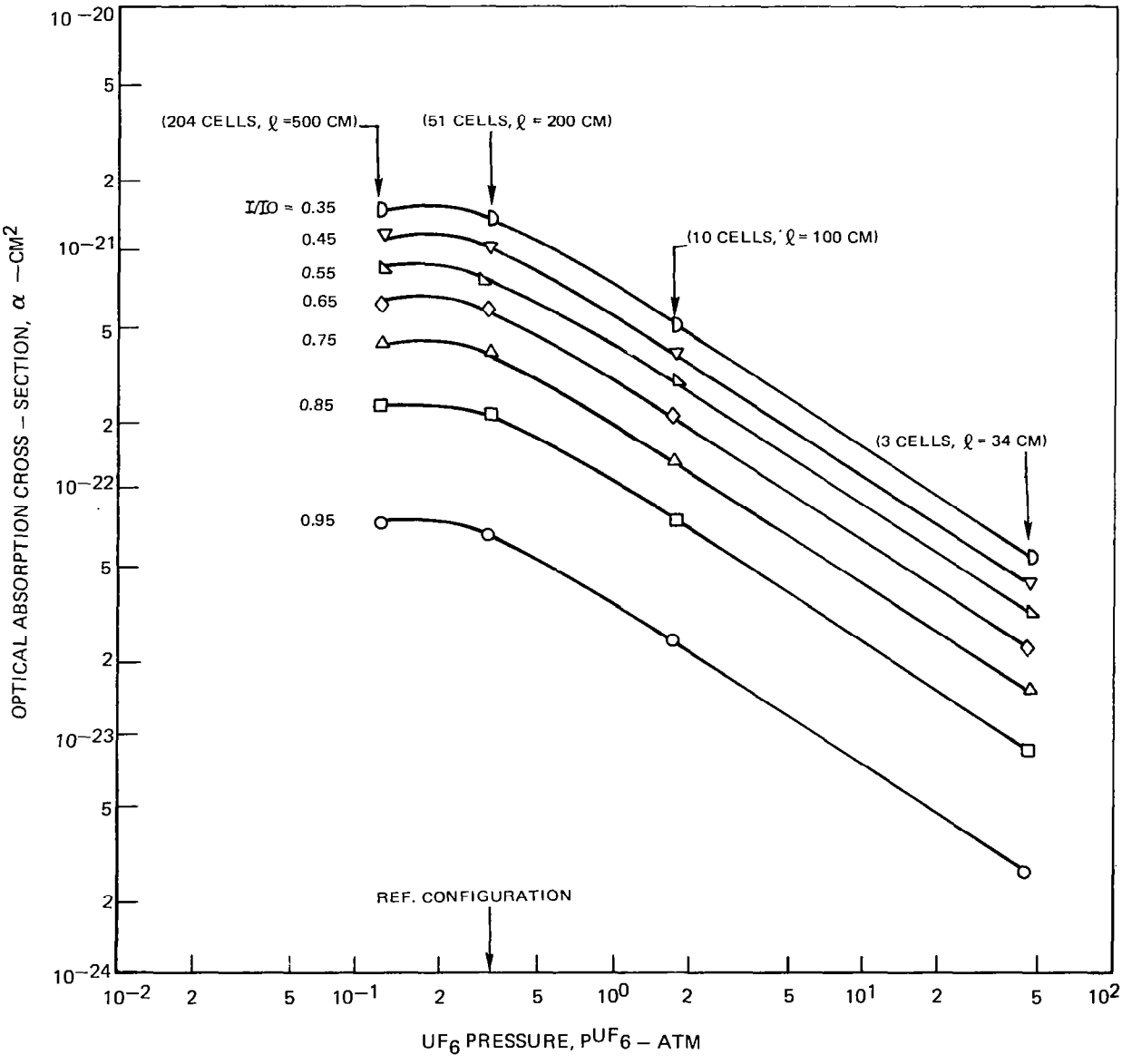

FIG. 18

VARIATION IN POWER AND FLUX WITH POWER DENSITY

M_{CRIT} = 4.9 K g U–235

P_{U-235} = 0.32 atm

ρ_{U-235} = 1.5 mg/cm^3

V_F = 3.2x10^6 cm^3

R_{CELL} = 10 cm

CORE LENGTH = 200 cm

NO. OF CELLS = 51

SONIC VELOCITY = 436 m/s

P_{He} = 3.4 atm

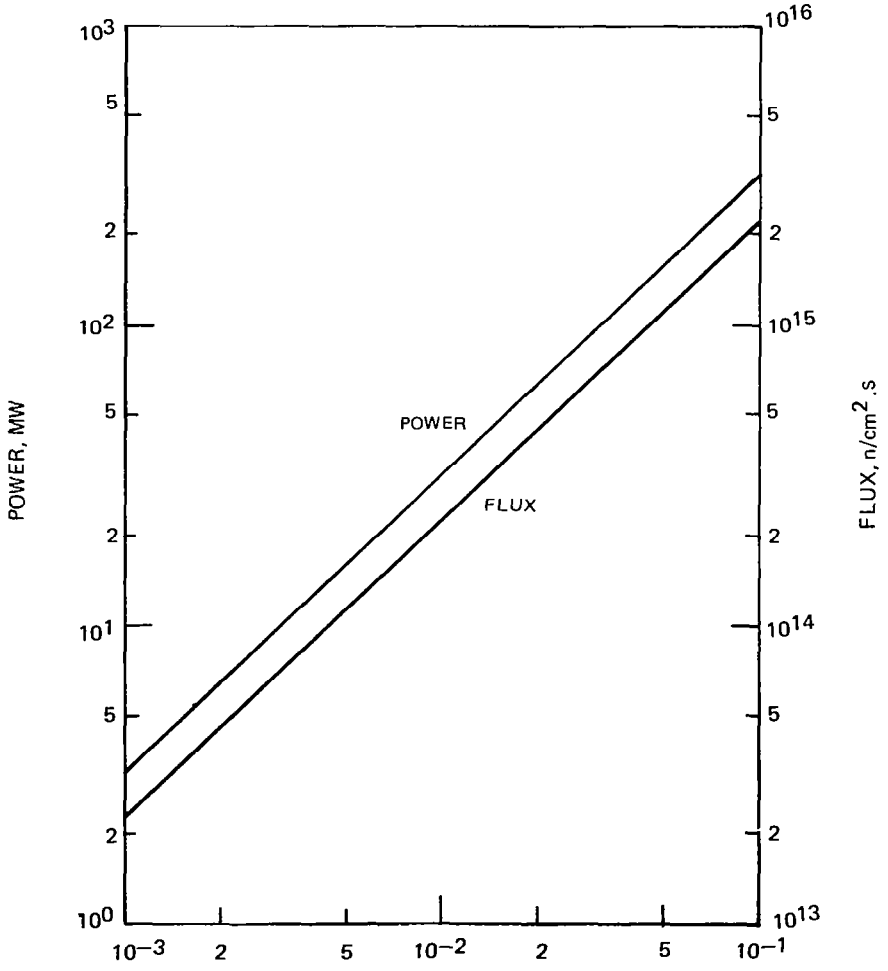

FIG. 19

VARIATION IN FLOW RATES WITH POWER DENSITY

M_{CRIT} = 4.9 Kg U–235

P_{U-235} = 0.32 atm

ρ_{U-235} = 1.5 mg/cm^3

V_F = 3.2x10^6 cm^3

R_{CELL} = 10 cm

CORE LENGTH = 200 cm

NO. OF CELLS = 51

SONIC VELOCITY = 436 m/s

P_{He} = 3.4 atm

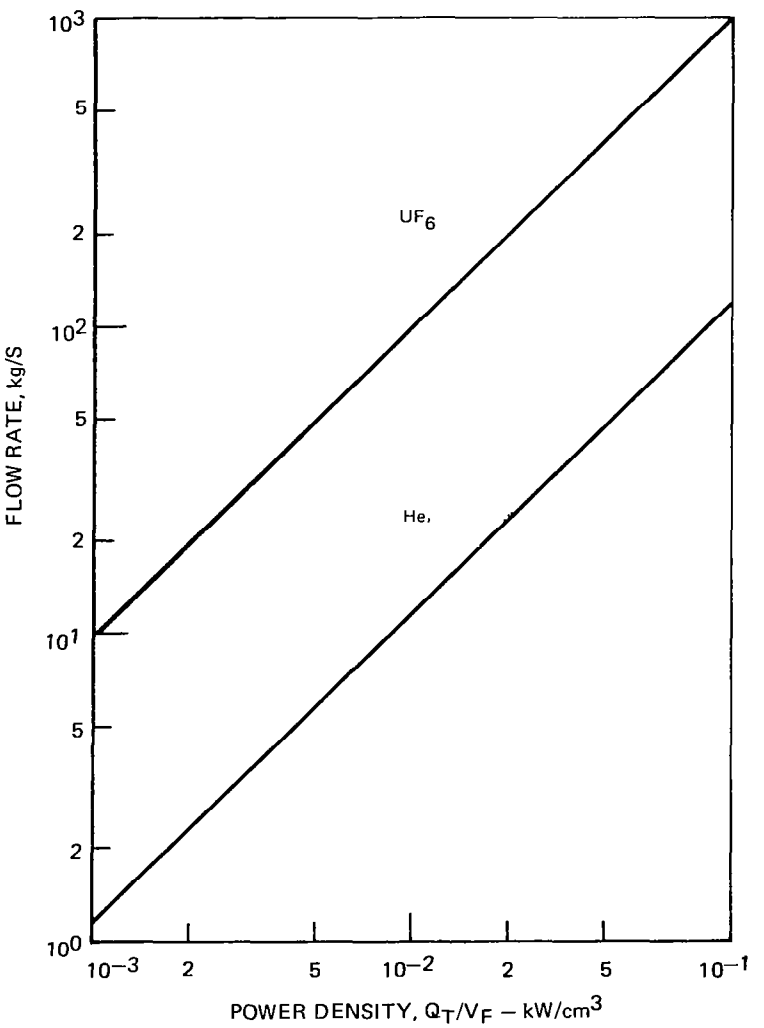

FIG. 20

VARIATION IN FUEL VELOCITY AND CAVITY RESIDENCE TIME WITH POWER DENSITY

M_{CRIT} = 4.9 Kg U–235

P_{U-235} = 0.32 atm

ρ_{U-235} = 1.5 mg/cm^3

V_F = 3.2x10^6 cm^3

R_{CELL} = 10 cm

CORE LENGTH = 200 cm

NO. OF CELLS = 51

SONIC VELOCITY = 436 m/s

P_{He} = 3.4 atm

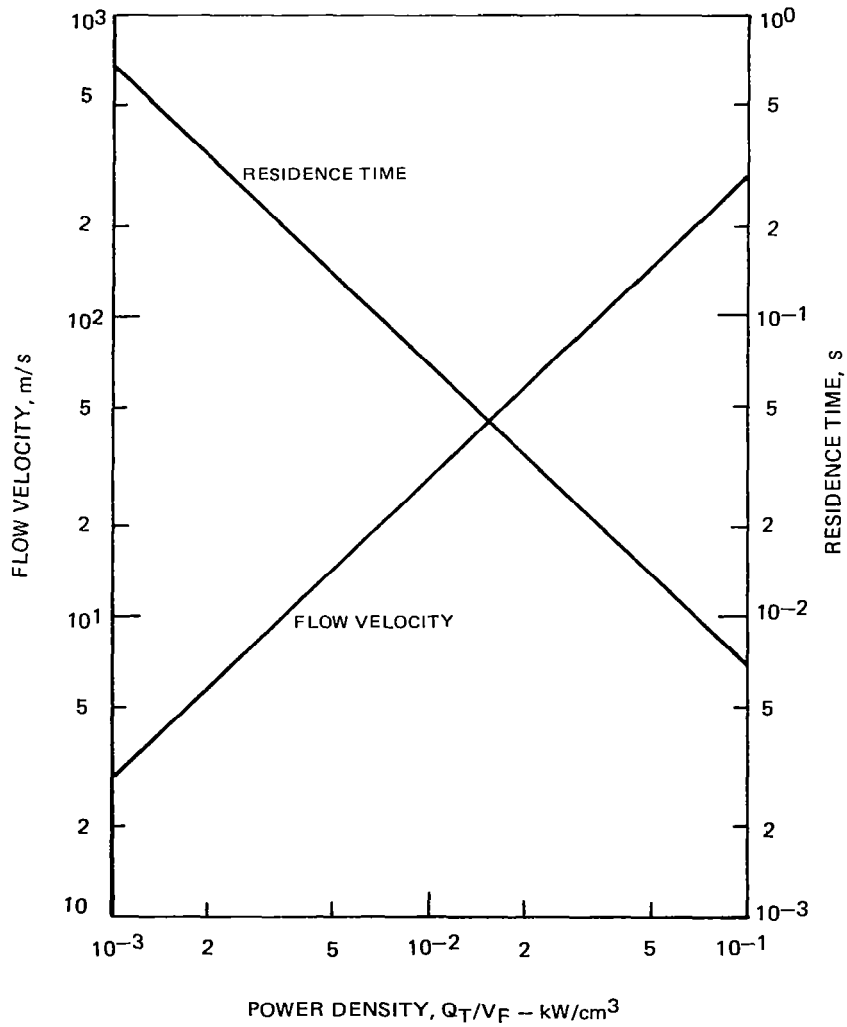

FIG. 21

CYCLE SCHEMATICS FOR NUCLEAR PUMPED LASER POWER EXTRACTION SYSTEMS

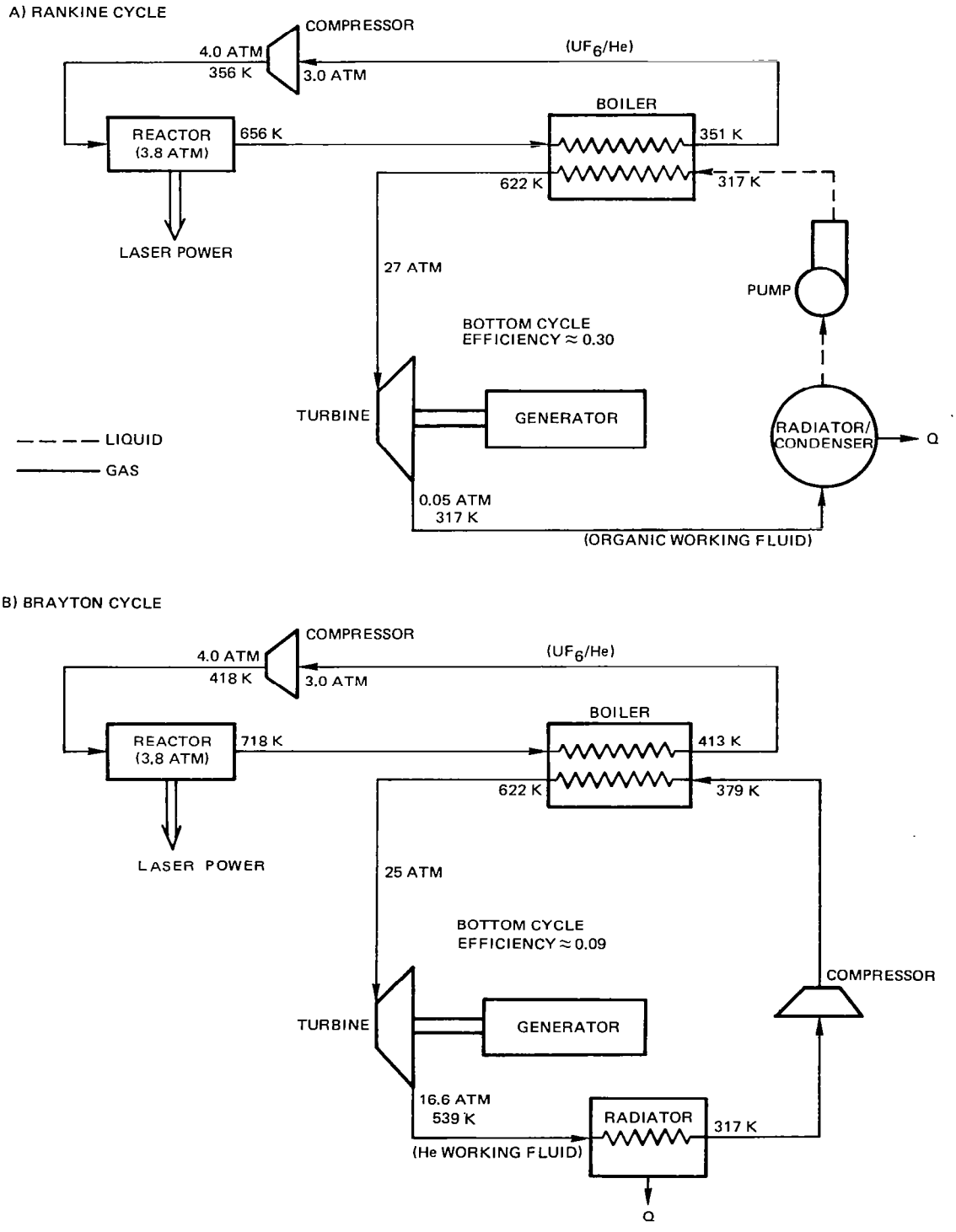

1. Report No.	2. Government Accession No.	3. Recipient's Catalog No.
NASA CR-3128		

4. Title and Subtitle	5. Report Date
Initial Conceptual Design Study of Self-Critical Nuclear Pumped Laser Systems	April 1979
	6. Performing Organization Code
7. Author(s)	8. Performing Organization Report No.
Richard J. Rodgers	
	10. Work Unit No.
9. Performing Organization Name and Address	
United Technologies Research Center East Hartford, Connecticut 06108	11. Contract or Grant No. NAS1-14329, Mod 3
	13. Type of Report and Period Covered Contractor Report
12. Sponsoring Agency Name and Address	
National Aeronautics and Space Administration Washington, DC 20546	14. Sponsoring Agency Code

15. Supplementary Notes

Project Manager, Frank Hohl, Space Systems Division, NASA Langley Research Center
UTRC Technical Program Manager: J. S. Kendall TOPICAL REPORT

16. Abstract

An analytical study of self-critical nuclear pumped laser system concepts was performed. Primary emphasis was placed on reactor concepts employing gaseous uranium hexafluoride (UF_6) as the fissionable material. Relationships were developed between the key reactor design parameters including reactor power level, critical mass, neutron flux level, reactor size, operating pressure, and UF_6 optical properties. The results were used to select a reference conceptual laser system configuration.

In the reference configuration, the 3.2 m^3 lasing volume is surrounded by a graphite internal moderator and a region of heavy water. Results of neutronics calculations yield a critical mass of 4.9 kg U^{235} in the form of $^{235}UF_6$. The configuration appears capable of operating in a continuous steady-state mode. The average gas temperature in the core is 600 K and the UF_6 partial pressure within the lasing volume is 0.34 atm.

17. Key Words (Suggested by Author(s))	18. Distribution Statement
Nuclear Pumped Laser Gas-Core Reactor Space Power Transmission	Unclassified-unlimited Subject Category 73

19. Security Classif. (of this report)	20. Security Classif. (of this page)	21. No. of Pages	22. Price*
Unclassified	Unclassified	48	$4.50

* For sale by the National Technical Information Service, Springfield, Virginia 22161

NASA-Langley, 1979